[AMERICAN JOURNAL OF SCIENCE, VOL. 322, APRIL, 2022, P. 533–560, DOI 10.2475/04.2022.01]

American Journal of Science

APRIL 2022

NEW IDRIA SERPENTINITE PROTRUSION, DIABLO RANGE, CALIFORNIA: FROM UPPER MANTLE TO THE SURFACE

ROBERT G. COLEMAN*,¶, JARED T. GOOLEY**,***,†, ROBERT T. GREGORY§,
and STEPHAN A. GRAHAM*

ABSTRACT. The New Idria serpentinite body in the Coast Ranges of California is a diapir that resulted from the interaction of the migrating Mendocino trench-ridge-transform fault triple junction, transpression, metasomatic fluids, and previously subducted oceanic crust and mantle. Northward propagation of the San Andreas fault progressively eliminated the original subduction zone, allowing seawater to penetrate into the formerly subducting abyssal peridotite mantle, triggering serpentinization. The associated physical changes in density, volume, and strength yielded an expanding, buoyantly rising serpentinite protrusion, facilitated by transpression along the San Andreas fault. Sedimentary facies and intrusion of minor cross cutting syenite and alkali basalt dikes indicate that the serpentinization-driven diapir buoyantly rose and widely breached the surface by *ca.* 14 Ma, attending migration of the Mendocino Triple Junction past the latitude of New Idria.

Key words: Serpentinite Protrusion, Peridotite, Metasomatism, San Andreas Fault, Mendocino Triple Junction

INTRODUCTION

The New Idria serpentinite body is an ellipsoidal serpentinite diapiric dome, 22 km long and 8 km wide, exposed between the San Andreas fault to the west and the San Joaquin Valley to the east (figs. 1, 2). It crops out in the southern Diablo Range at the structural and topographic culmination of the NW-SE trending Coalinga anticline, lying between the Vallecitos syncline to the northeast and the Avenal syncline to the southwest. Its greatest elevation is nearly 1600 m at San Benito Mountain, towering over the adjacent San Joaquin Valley sitting at about 70 m above sealevel. The Coalinga anticline plunges southeast into the subsurface, but the fold-form continues southward, where it is expressed as Kettleman North Dome. Oil was discovered in folded uppermost Cretaceous strata on Coalinga anticline in 1890 (Anderson, 1952), followed over the past 125 years by extensive drilling and reflection seismic surveys across the Coalinga region. Together, outcrop and subsurface data form the basis for reconstructing a detailed stratigraphic and erosional history of the emplacement of the New Idria serpentinite dome (Anderson and Pack, 1915; Arnold and Anderson, 1910; Bramlette, 1946; Casey and Dickinson, 1976; Carlson and others, 1984; Bate, 1985; Dibblee and others, 1999). New Idria is the largest of a number of similar

---

* Department of Geological Sciences, Stanford University, Stanford, California 94305, USA
** Geology, Energy & Minerals Science Center, U.S. Geological Survey, Reston, Virginia 20192, USA
*** Previously Department of Geological Sciences, Stanford University, Stanford, California 94305, USA
§ Department of Geological Sciences, Southern Methodist University, Dallas, Texas 75275, USA
¶ Deceased, October 18, 2020.
† Corresponding author: jgooley@usgs.gov

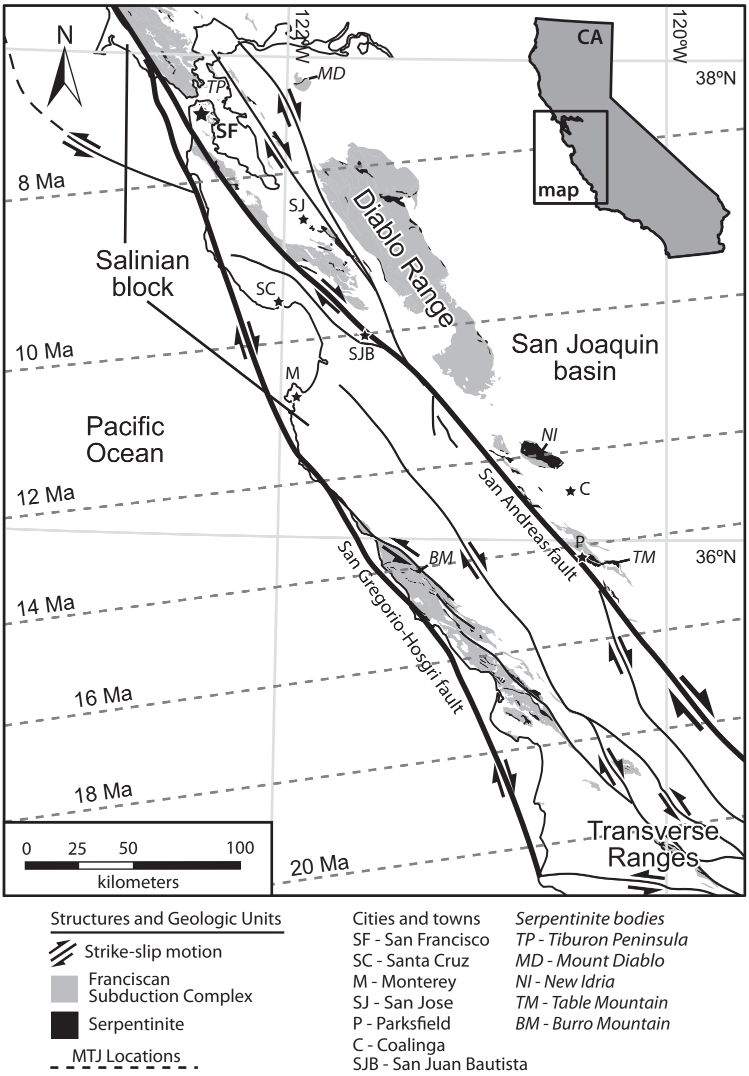

Figure 1. Map of central California showing principal serpentinite bodies and faults discussed in the text. Dashed lines are approximate paleolatitudes of the Mendocino Triple Junction from Stock and Molnar (1988).

serpentinite bodies that crop out adjacent to the San Andreas fault, from Table Mountain in the south, to the Tiburon Peninsula in the north (fig. 1).

The Coalinga Earthquake of 1983, which occurred 25 km southeast of the New Idria serpentinite dome on a blind thrust beneath Coalinga anticline, was studied intensely by the United States Geological Survey (USGS), providing new geophysical parameters demonstrating that the New Idria serpentine body extends at least 10 km below the surface (Rymer and Ellsworth, 1990). Seismic, magnetic and gravity data revealed that at this depth the dome consists of serpentinized peridotite (~40%) with reduced seismic velocity and specific gravity. Continuing metasomatic (rheological) weakening and expansion of the serpentinized abyssal peridotite (Warren, 2016) facilitated its upward, aseismic, plastic ascent (Wentworth, 1990; Tsujimori and others, 2007a; Moore and Lockner, 2013) (fig. 3).

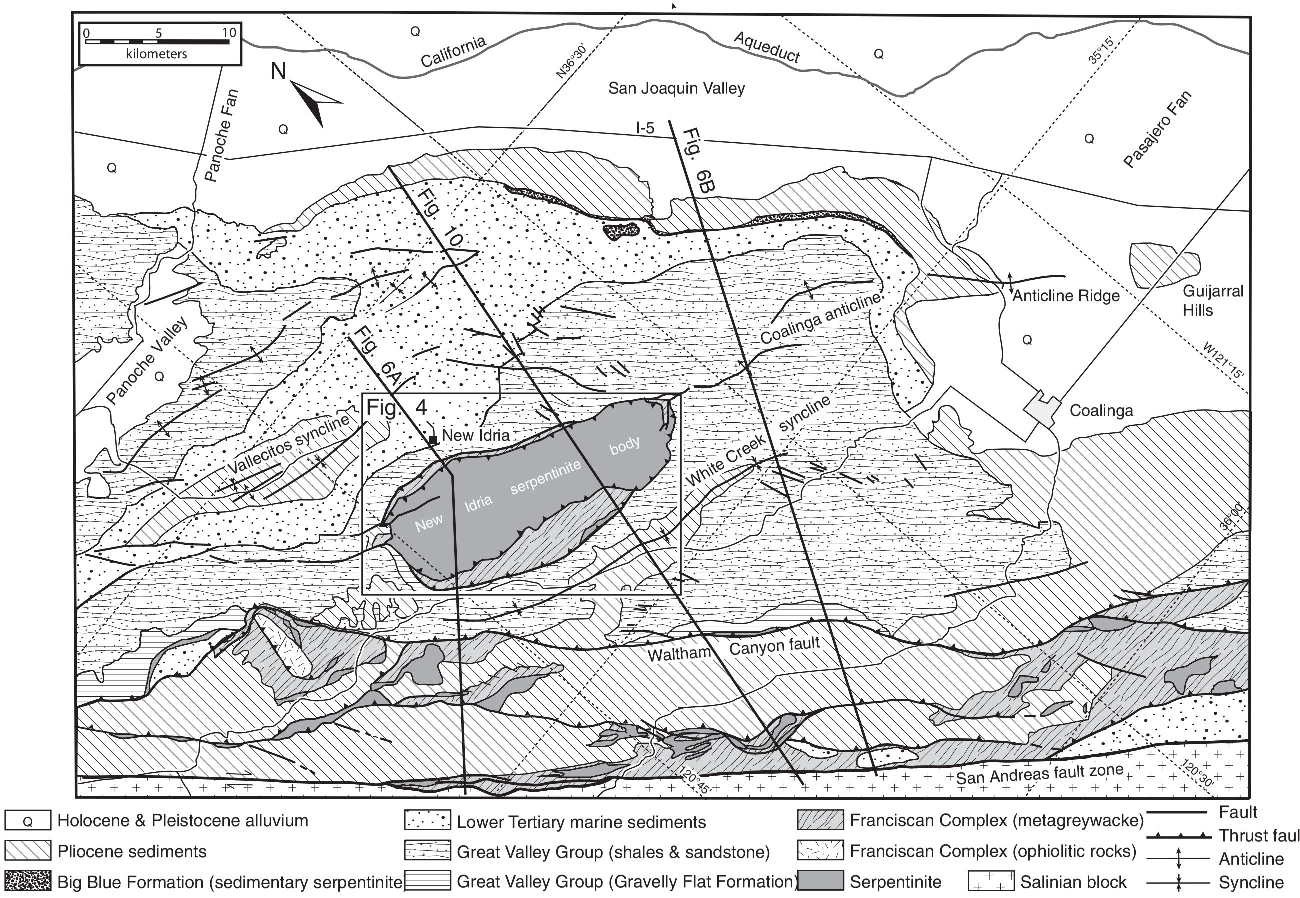

Figure 2. Geologic map of the New Idria serpentinite protrusion and surrounding area in the Diablo Range of central California. The serpentinite diapir occupies the crest of the Coalinga antiform and surrounding faults mark the exhumed trace of the Coast Range fault. Modified from Tsujimori and others (2007a).

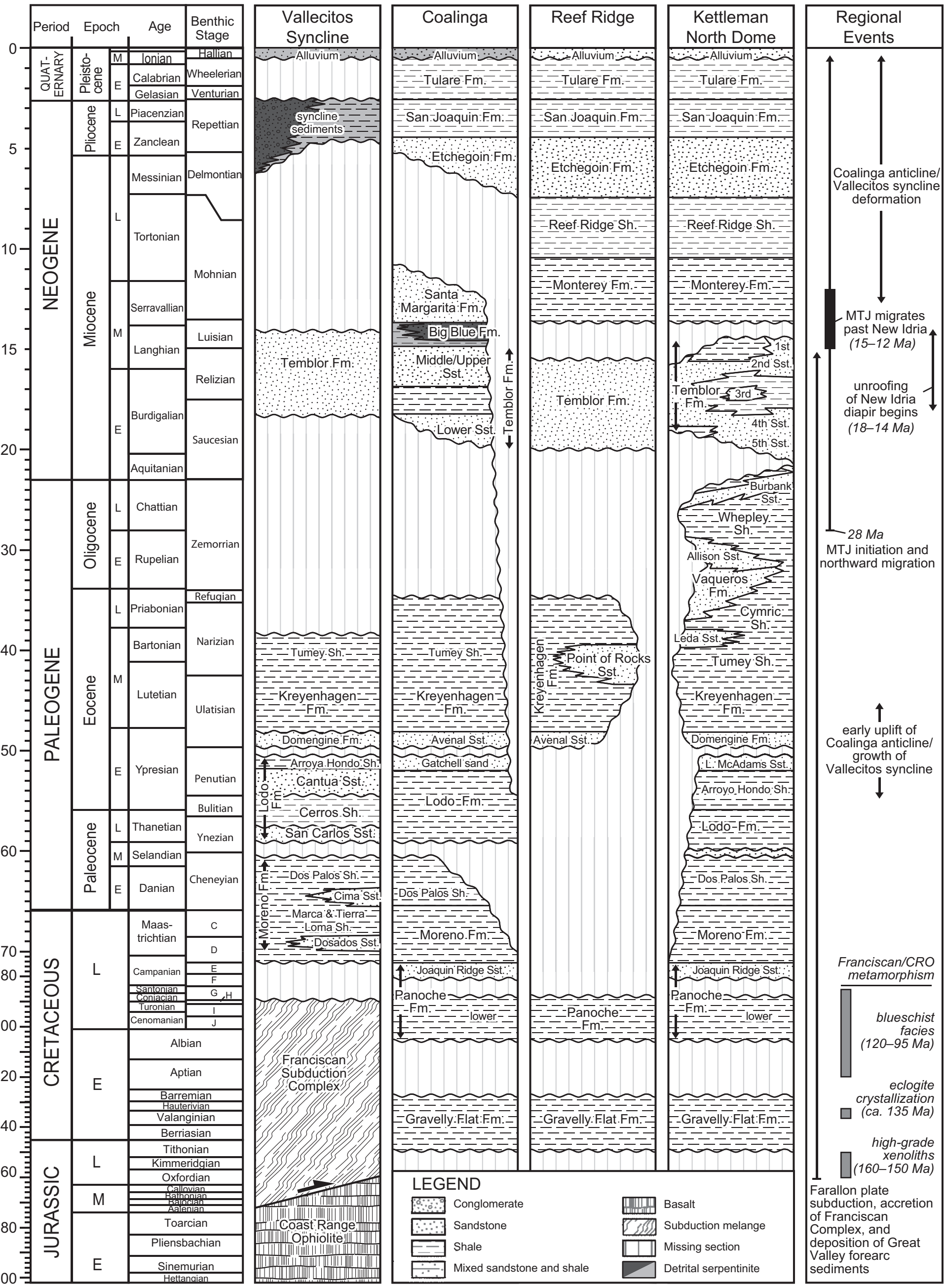

Figure 3. Stratigraphic correlation, lithostratigraphy, and timing of regional events near the New Idria serpentinite diapir. Note time scale changes at 20 Ma and 70 Ma. Modified from Bate (1985); Cooley (1985); Kuespert (1985); Rentschler (1985); Bloch and others (1993); Nilsen and Moore (1997); Scheirer and Magoon (2006); Johnson and Graham (2007); Sharman and others (2017).

Following the definition of Lockwood (1971), the New Idria massif is a serpentinite protrusion. Use of the term ‘protrusion’, instead of ‘intrusion’ emphasizes a process that highlights the difference between ultra-high temperature processes involving ultramafic magmas versus low-temperature processes involving metasomatic (Zharikov and others, 2007) and rheologic changes during serpentinization. The history of the diapir spans nearly 170 m.y. from the Jurassic, when its ultramafic rocks formed as part of the oceanic Kula plate, to the present. Serpentinite protrusions, formerly mapped as products of altered igneous ultramafic intrusions, are now known to be metasomatized abyssal mantle peridotite (Lockwood, 1971). Metasomatism facilitates serpentinization, resulting in expansion up to ~40% within the peridotite, a loss of density that enhanced buoyancy, and a loss of rheological strength (Andreani and others, 2007; Bach and others, 2012; Bayrakci and others, 2016). The initiation of the San Andreas transform fault promoted deep penetration of seawater driving the serpentinization and enabled the formerly high-density mantle to flow upward, decoupling it from the overlying dense mafic (basalt-gabbro) Kula oceanic crust. The surface exposures are a mixture of fragmented serpentinite (95%), a mélange that forms a huge deposit of short fiber chrysotile asbestos (Ross and Nolan, 2003) containing 5% inclusions of metamorphic rocks (eclogite, blueschist, amphibolite, andradite-bearing antigorite serpentinite and Franciscan mélange). Rare boulders of the original abyssal peridotite protolith are exposed in stream terraces.

In this paper, we review the geologic setting of the protruding serpentinite, its petrologic characteristics, the tectonics of xenolithic rocks, the rheological properties of the protrusion, and the sedimentary and stratigraphic record of associated strata. These data help constrain the roles of Mendocino Triple Junction (MTJ) migration and accompanying thrusting and folding of the San Andreas transform margin. In aggregate, these processes combined to bring the New Idria serpentinite body to the surface (Suzuki, 1986; Vermeesch and others, 2006; Titus and others, 2007; Moore and Lockner, 2013).

TECTONIC HISTORY OF CENTRAL CALIFORNIA

Much of the tectonic history of central California can be attributed to two phases. First, Late Jurassic to Eocene time, subduction of the Farallon plate beneath the North American plate produced one of the most well studied convergent margins in the rock record (Ingersoll, 1982). Elements of this convergent margin consist of the Sierra Nevada magmatic arc, the Great Valley forearc basin, and the Franciscan accretionary wedge and obducted Coast Range Ophiolite that comprises much of the Coast and Diablo Ranges today (fig. 1). Oblique convergence of the Kula-Farallon and North American plates persisted until collision of the East Pacific Rise with the North American convergent margin, forming the MTJ around *ca.* 28 Ma (Atwater, 1970; Atwater and Molnar, 1973; Dickinson and Snyder, 1979; Atwater, 1989). In this second tectonic regime, the newly developed right-lateral San Andreas transform plate boundary and subsidiary strike-slip faults dissected the remnant elements of the Mesozoic convergent margin and translated the newly established Salinian block northward by approximately 360 km or greater since *ca.* 23 Ma (Sharman and others, 2013; Gooley and others, 2021b). As a result of northward migration of the southern terminus of the subducting slab (fig. 1), arc magmatism and associated volcanic detritus that was shed into the basin was progressively shut off (Graham and others, 1984; Gooley and others, 2021a). Transpression along the central segment of the San Andreas fault caused folding and uplift of Franciscan and overlying Mesozoic–Cenozoic basin strata (fig. 3), in which numerous isolated serpentinite bodies have been emplaced (fig. 1). Tsujimori and others (2007a) summarized the possible protoliths of the New Idria serpentinite body. While the protolith has generally been regarded as abyssal peridotite from the Kula plate (Coleman, 1996), as explained below, other models with supporting evidence have been presented for possible dismembered Coast Range Ophiolite or serpentinized forearc mantle wedge (Lazar and others, 2021). While clues to the geologic origins of the New Idria diapir continue be revealed, here we synthesize the petrologic, stratigraphic, geophysical, and structural constraints on the metasomatism of peridotite and emplacement, uplift, and exhumation of the New Idria serpentinite diapir.

NEW IDRIA SERPENTINITE BODY: PETROLOGIC CONSTRAINTS

The New Idria serpentinite body contains mainly highly sheared, crushed and incoherent material that is made up of soft, crumbly aggregates and sheets of serpentine asbestos (fig. 4) (Mumpton and Thompson, 1975). The serpentinite contains up to 60 percent chrysotile (asbestos) associated with lizardite, brucite, and magnetite; the rare occurrences of abyssal mantle peridotite protolith consist of olivine, clinopyroxene, orthopyroxene, and chromite. The serpentinite has little strength at the surface, and landforms that develop on it are easily eroded into rounded hills.

The few occurrences of abyssal peridotite preserved within the New Idria serpentinite contain remnants of original mantle mineral assemblages. The latter are typical of depleted harzburgite common in some of the less serpentinized peridotites of the California Coast Ranges (Loney and others, 1971; Graymer and others, 2014). Petrologic studies (Coleman, 1971, 1980a, 1980b, 1996) of California peridotites show that

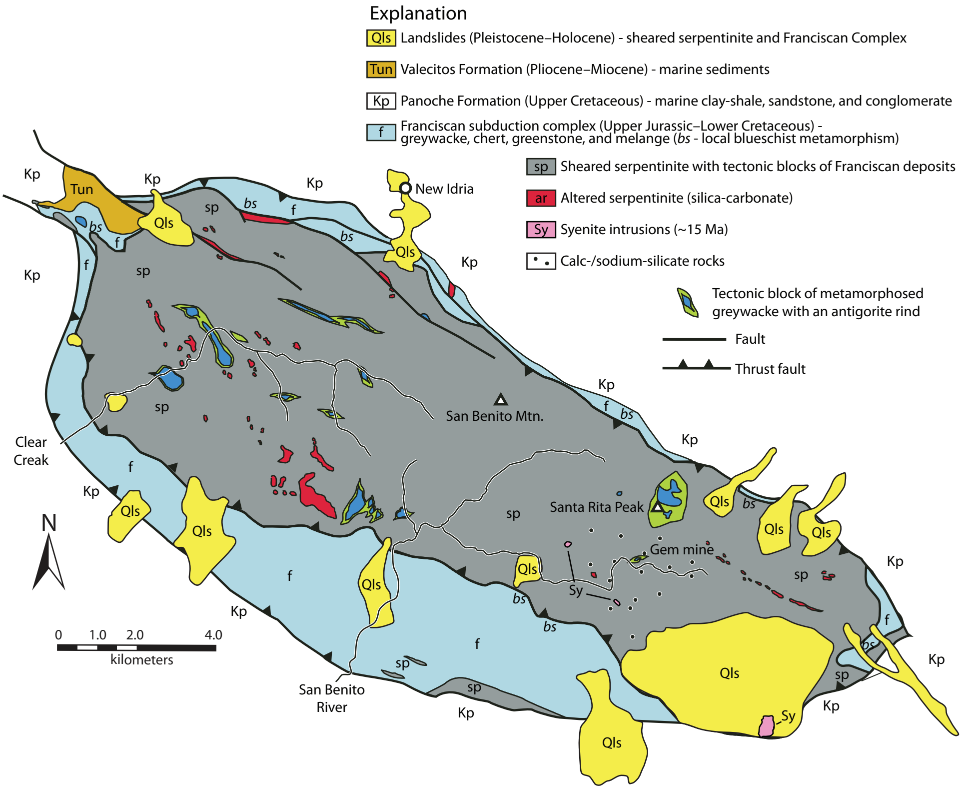

Figure 4. Detailed map of xenolithic inclusions, metasomatic replacement bodies, igneous intrusive syenite, alkali basalt, barium-titanium rich minerals (for example, benitoite), silica-carbonate veins (cinnabar) in the New Idria serpentine body. Antigorite rinds around tectonic inclusions have been exaggerated for clarity. All of the Franciscan tectonic inclusions in the mélange have undergone varying intensities of blueschist metamorphism. Low-grade blueschist metamorphism is sporadically developed in Franciscan greywacke surrounding the serpentinite body. Blueschist-eclogite and garnet amphibolite tectonic xenoliths are rare and are only found as rounded cobbles in Clear Creek. Adapted from Coleman (1996).

harzburgite is the main mantle protolith, with smaller amounts of dunite. Only rarely is clinopyroxene present, explaining the low silica activity during the main phases of serpentinization. Reddish-brown ribs of silica-carbonate rock within the New Idria serpentinite body developed during a very late-stage hydrothermal event that produced the mercury deposits once mined at the town of New Idria (Eckel and Myers, 1946).

The New Idria serpentinite contains numerous tectonic xenolith inclusions, several up to 1500 meters in length, as well as many others less than a meter in diameter (fig. 4). Santa Rita Peak exposes one of the largest tectonic inclusions, made up of mostly of antigorite serpentine with accessory andradite garnet and minor magnetite. This inclusion is typical of an earlier, deeper level serpentinization event in which jadeite formed at $P > 0.8$ GPA at T= 200–400 °C (Tsujimori and others, 2007b). These inclusions have a random distribution within the serpentinite body and their internal metamorphic fabrics distinctly differ from one inclusion to another (Coleman, 1961; Tsujimori and others, 2007a). The elongation of the larger jadeite-bearing inclusions exposed along Clear Creek are roughly parallel to the axis of the Coalinga anticline. These inclusions are commonly rimmed by highly sheared antigorite serpentine rinds, in contrast to the main serpentinite body that consist of flaky incoherent chrysotile-lizardite-brucite-magnetite assemblages.

Some contacts between the inclusions and the serpentinite bear evidence of a period of calcium metasomatism (rodingite assemblages) at an earlier stage of development. Although tectonic inclusions within the New Idria serpentinite exhibit some tendency of elongation toward parallelism with the shape of the protrusion, internal fabrics of the inclusions have random structural attitudes discordant to the plane of elongation of the host body. These tabular and elongate shapes, combined with steep dips of the bounding faults, suggest that they developed during the upward squeezing of the semiplastic serpentinite protrusion.

The newly formed serpentinite expanded upward, exhuming tectonic xenolith inclusions from the truncated Franciscan mélange. Continued incorporation of tectonic inclusions since middle Miocene time within the serpentinite diapir has preserved a historical record of dynamic rheomorphic and metasomatic events (fig. 5). These tectonic inclusions represent diverse rock types, and all specimens examined have undergone metamorphism of different intensities, including rare eclogites. The protolith for some of these inclusions, such as mafic volcanic-pyroclastic rocks, graywacke, chert, and shale, contain blueschist mineral assemblages consisting of chlorite, glaucophane, pumpellyite, albite, jadeite and stilpnomelane, can be traced to the Franciscan mélange. Rare occurrences of gneissic amphibolite and eclogite occur as small boulders in Clear Creek (Coleman, 1957; Tsujimori and others, 2007a).

The wide range of P/T parameters exhibited by these metamorphic xenolithic blocks supports the idea that the New Idria serpentinite diapir captured these blocks at various crustal levels and at different times during its expanding ascent (fig. 5). Ages of blueschist facies rocks within the Franciscan Complex range from 95 to 120 Ma (Wakabayashi, 2015). The less abundant higher-grade tectonic blocks, including eclogite within the serpentinite, range in age from 150 to 160 Ma (Mattinson and Echeverria, 1980; Mattinson, 1986, 1988; Moore and Blake 1989; Mattinson and Hopson, 1992; Wakabayashi and others, 2010; Ukar and others, 2012). The younger blueschist represents large coherent areas of metagraywacke and metabasalt recrystallized during subduction of the Franciscan forearc mélange during middle to Late Cretaceous times. In contrast, the higher-grade rocks, such as blueschist and eclogite, have Tithonian to Kimmeridgean ages and are much smaller than the individual xenolithic tectonic blocks that have a talc-actinolite or antigorite rinds recording their upward transport within serpentinite (Coleman and Lanphere, 1971; Coleman, 1980a; Wakabayashi and others, 2010; Ukar and others, 2012).

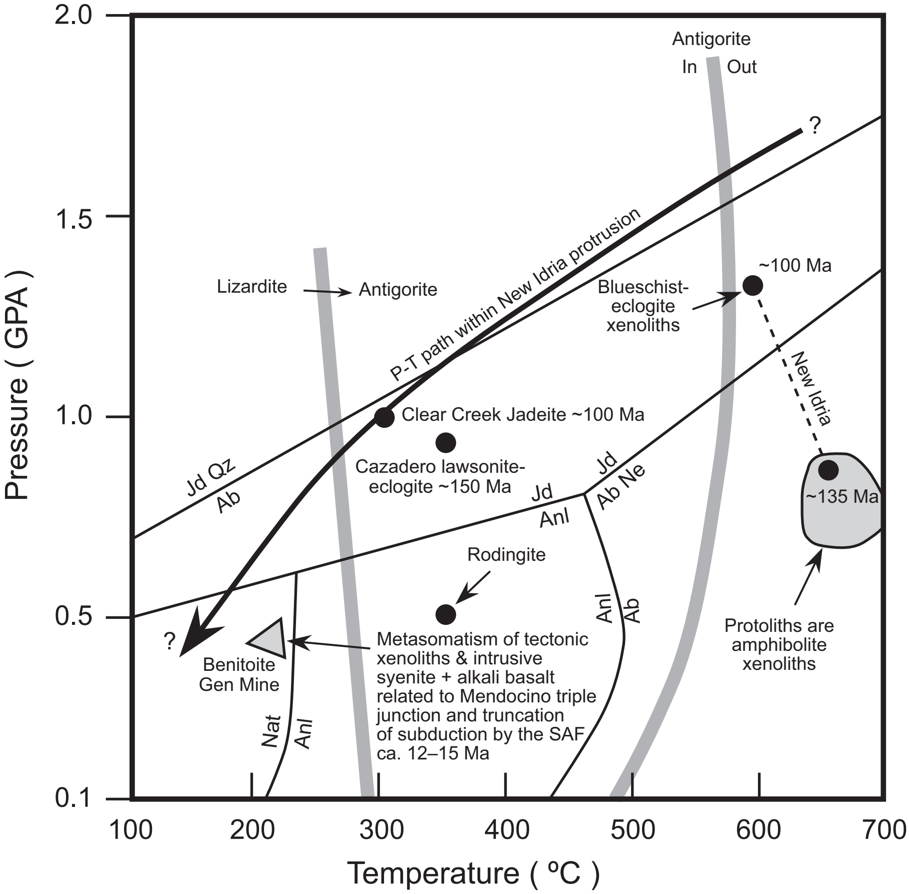

Figure 5. Estimated temperatures, pressures, and radiometric ages for xenolithic blueschist, amphibolite and eclogite rocks associated with endogenous metasomatites within the New Idria serpentine protrusion. Data for New Idria and Clear Creek jadeite from Tsujimori and others (2007a, 2007b); Cazadero eclogite (Shibakusa and Maekawa, 1997). Benitoite with calcium-sodium-titanium metasomatites and associated syenite and alkaline basalt intrusions (Obradovich and others, 2000; Van Baalen, 1993; Laurs and others, 1997). Na metasomatism (rodingite) in serpentine estimated from NaCl fluid inclusions and CH_4 (methane) (Normand and Williams-Jones, 2007). Rheological laws for natural serpentinites from Amiguet and others (2012).

The discovery of peridotite, eclogite and amphibolite retrograded assemblages within the New Idria serpentine mélange confirms the notion that the serpentine was derived from peridotites in the upper mantle. The eclogite crystallized at T = 580–620°C at P >1.0 GP and the amphibolite T = 630–680 °C at P = 0.8–1.0 GPa (K-Ar 135 +/− 7 Ma) with retrograde blueschist T = 200–290°C at P = ~0.5 GPa (Tsujimori and others, 2007a). The Coyote Hills serpentine protrusion at the intersection of the Hayward–Calaveras faults near San Jose (fig. 1) was invaded by alkaline basalt dikes bearing mantle xenoliths. Titus and others (2007) estimated the P/T range for spinel lherzolite xenoliths within the Coyote Lake alkali basalt equilibrated at 970 to 1700 °C within a mantle shear zone at depths 38 to 43 km that connects upward with the San Andreas fault system. Numerous other alkali basaltic eruptions track the northward migration of the Mendocino Triple Junction and are related to the developing San Andreas transform system (McLaughlin and others, 1996; Furlong and Schwartz, 2004).

These new data allow a regional connection with blueschist facies subduction ages for Franciscan mélange in California Coast Ranges and Klamath Siskiyou Mountains (Coleman and Lanphere, 1971; Ghent and Coleman, 1973; Ukar and others, 2012). Metamorphism within the Franciscan mélange under higher temperatures produced a retrograde younger PT path within the rising serpentinite diapir. These diverse PT paths are sometimes considered to be the result of refrigeration or counter-clockwise PT movements within the serpentinite protrusions, rather than random subsurface tectonic capture of the high-grade blocks into the rising weak, viscous serpentine protrusions (Horodyskyj and others, 2009).

HYDRATION OF PERIDOTITE

The rheologic changes in density (-), volume (+), and strength (-) within the parental peridotite to serpentinite are impressive (Gerya and others, 2002; Christensen, 2004; Herzberg, 2004; Bach and others, 2012; Germanovich and others, 2012; Evans and others, 2013; Rouméjon, and Cannat, 2014). At Moho depths, the protolith was transected by the vertical San Andreas fault and the first stages of serpentine metasomatism began. Eastward and upward transport within the Franciscan mélange culminated in the middle Miocene (fig. 6). The hydration of the New Idria peridotite to serpentinite is a retrogressive metasomatic (metamorphic) chemical reaction that can be described in simple terms (Martin and Fyfe, 1970; Mumpton and Thompson 1975; Lowell and Rona, 2002; Escartín and others, 2001), as follows:

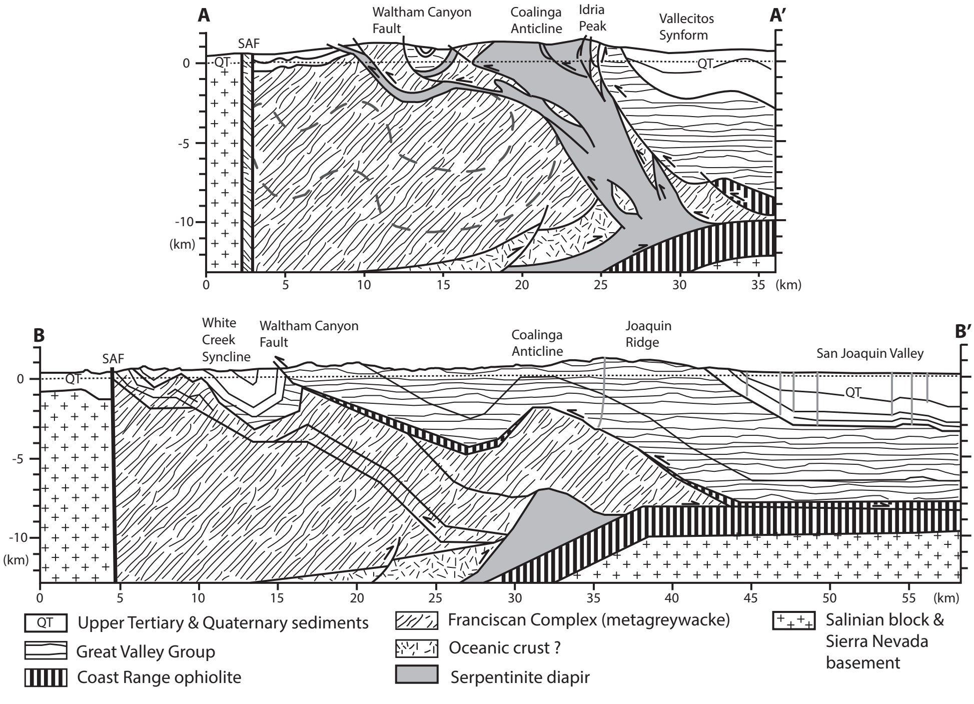

Figure 6. Structural cross-sections showing truncation of the Franciscan mélange wedge by the San Andreas fault to the west and protrusion of the serpentinite upward aided by blind thrusting beneath and into Great Valley forearc strata. Adapted from Namson and others (1990) and Coleman (1996). Lines of sections shown on figure 2.

$$\underset{\text{forsterite}}{2\mathrm{Mg_2SiO_2}} + \underset{\text{water}}{3\mathrm{H_2O}} \rightarrow \underset{\text{serpentine}}{\mathrm{Mg_3Si_2O_5(OH)_2}} + \underset{\text{brucite}}{\mathrm{Mg(OH)_2}}\underset{\text{water}}{(13\text{–}14\ \text{wt\%}\ \mathrm{H2O})} \tag{1}$$

Serpentinization is an exothermic chemical reaction at estimated temperatures up to ~300 °C (Fyfe and Lonsdale, 1981). The evidence of increasing temperature for the New Idria protrusion exists along the serpentinite contact with the overlying shale, which preserves thermal transformation of disordered silica (opal) diatom skeletons to ordered silica polymorphs (quartz), which are controlled primarily by temperature >80 °C (Murata and others, 1979). Furthermore, Vermeesch and others (2006) observed high vitrinite reflectance values in Great Valley Group strata near the contact with the New Idria serpentinite body, and partial to complete annealing of detrital apatite fission tracks at *ca.* 14 Ma that they associated with development of a middle Miocene thermal halo around the rapidly emplaced diapir.

The earliest serpentinization of the New Idria diapir was initiated by the incursion of marine water whose pH likely rose to 10–12 during metasomatism of peridotite (Barnes and others, 1972; Moody, 1976). The metasomatic evolution of the New Idria serpentinite body involves aseismic interaction between deformation, fluid infiltration, and multiple metasomatic fluid reactions (Bezacier and others, 2013). These changes occurred over geological time scales (~1–15 Myr) within a weak, plastic, and expanding serpentinized abyssal peridotite mass.

EMPLACEMENT OF THE NEW IDRIA SERPENTINITE BODY

Stratigraphic Constraints

A key piece of evidence for the timing of principal emplacement and unroofing of the New Idria serpentinite body is the upper middle Miocene Big Blue Formation, an areally and temporally restricted sedimentary unit consisting overwhelmingly of detrital serpentinite, which crops out for about 30 km along the east flank of Coalinga anticline and the western margin of the San Joaquin Valley (figs. 2 and 3). Initial unroofing of the serpentinite diapir began during deposition of the underlying middle Miocene Temblor Formation (14–18 Ma; Scheirer and Magoon, 2006), based on local lenses of serpentinous detritus within the arkosic Temblor Formation documented in the subsurface of Coalinga oil field (Bate, ms, 1984, 1985). The Big Blue Formation is unfossiliferous, but is inferred to be late middle Miocene in age (Luisian provincial benthic foraminiferal stage, Casey and Dickinson, 1976; 13.5–15 Ma, using the time scales of Johnson and others, 2005 and McDougall, 2007). The Big Blue is bracketed by the biostratigraphically well-constrained fossiliferous Temblor Formation below and the Santa Margarita Formation above. By virtue of its distinctive character, the Big Blue Formation was recognized early in the geologic investigation of the Coast Ranges (Arnold and Anderson, 1910; Anderson and Pack, 1915; Adegoke, 1969). Subsequent workers (Casey and Dickinson, 1976; Casey, 1984; Bate, ms, 1984, 1985; Beery, ms, 1988) documented its sedimentary characteristics, facilitating an understanding of the timing of New Idria emplacement and the associated paleogeography.

Although the Big Blue Formation records extensive surface breaching of the New Idria serpentinite body, stratigraphic and petrologic evidence indicates that Coalinga anticline began to develop by the Cretaceous. McGuire (1988a, 1988b) noted rare clasts of red radiolarian chert derived from the Franciscan Complex in Maastrichtian strata in the Coalinga region. The upper Paleocene–lower Eocene Cantua Sandstone is a deep-marine turbiditic unit stratigraphically confined to the Vallecitos syncline (fig. 7), paired with and adjacent to the Coalinga anticline to the northwest (Nilsen

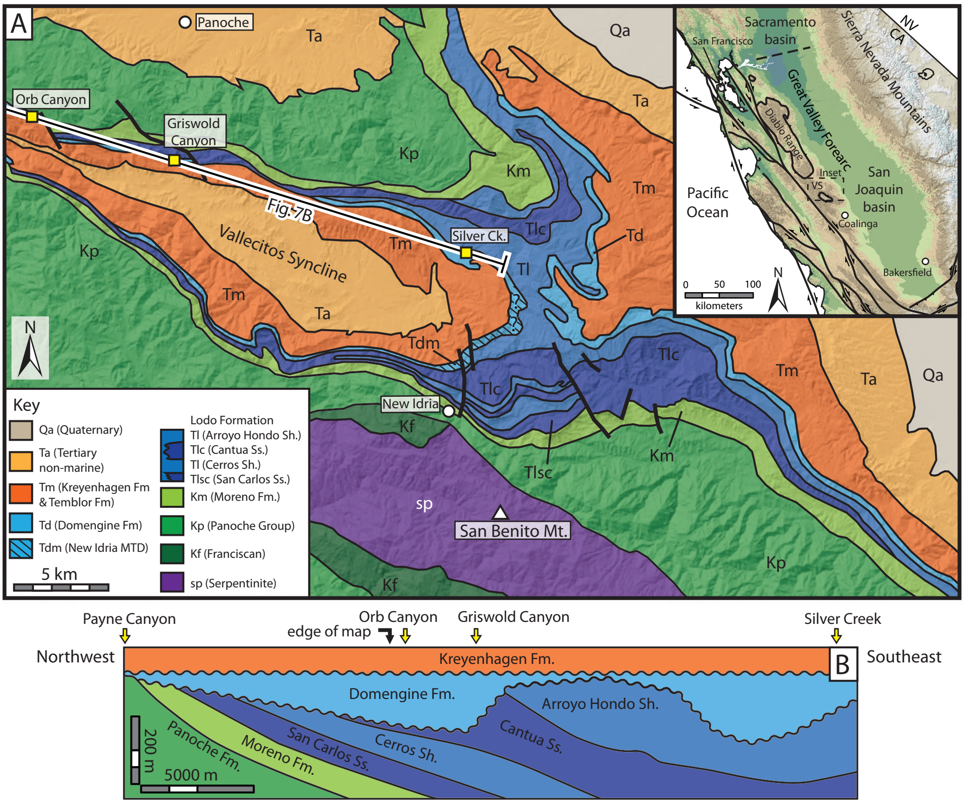

Figure 7. (A) Geologic map of the paired Vallecitos syncline and New Idria antiform illustrating structural confinement of the syn-tectonic Cantua Sandstone (TK, dark blue). (B) Generalized cross section along the northern flank of the Vallecitos syncline through stratigraphic sections indicated on map and cross section and continuing several kilometers to the west of the map boundary, showing stratal truncation beneath sub-Domengine (middle Eocene) angular unconformity that documents Eocene growth of the Vallecitos syncline and New Idria anticline. Modified from Sharman and others (2017).

and others, 1974; Graham and Berry, 1979; Anderson, 1996). Subsequently, the limbs of the Vallecitos syncline were uplifted and erosionally beveled deeply into Upper Cretaceous forearc strata (fig. 7). The presence of red radiolarian chert pebbles in the middle Eocene Domengine Formation at the western end of the Vallecitos syncline (Schulein, ms, 1993; Sharman and others, 2017) indicates that Cretaceous forearc strata were completely eroded and Franciscan subduction complex rocks were exposed and provided detritus to Vallecitos syncline by at least middle Eocene time. The upper lower to middle Miocene Temblor Formation exposed across Coalinga anticline includes nonmarine to shallow marine sandstone whose facies, paleocurrents and petrology (Bate, 1985; Bent, 1985) demonstrate that the Cretaceous forearc strata and Franciscan rocks continued to be unroofed in up-plunge portions of Coalinga anticline (fig. 8). In sum, an ancestral Coalinga anticline existed at least 50 Myr prior to Big Blue Formation sedimentation, and we thus speculate that the preexistent Coalinga anticline likely served as a Miocene structural guide for localizing the ascending New Idria body.

The Big Blue Formation and overlying upper Miocene Santa Margarita Formation are truncated across the breadth of the down-plunge end of Coalinga anticline by a

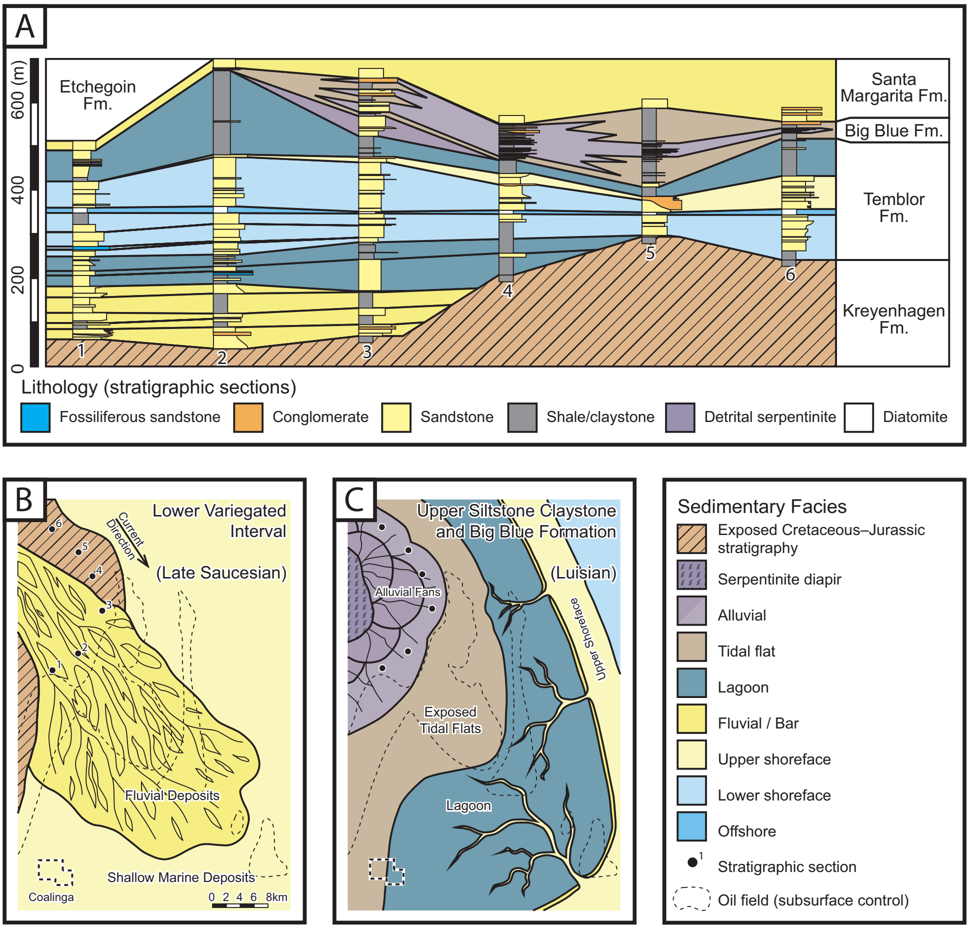

Figure 8. Lithostratigraphy and paleogeography of the Temblor and Big Blue formations on Coalinga anticline. (A) Lithostratigraphy from stratigraphic measured sections; (B) Paleogeography and depositional environments of the lower Temblor Formation on cross-section A; (C) Paleogeography and depositional environments of the Big Blue Formation on cross-section A. Redrawn from Bate (ms, 1984, 1985).

latest Miocene-early Pliocene unconformity that locally truncates the entire Cenozoic section (fig. 3). This unconformity likely reflects accelerated uplift and shortening of the eastern Coast Ranges (Namson and others, 1990), perhaps due to a change in pole of rotation of the Pacific-North America plate pair (Miller and Graham, 2018). Subsequent deposition occurred in the form of the shallow marine-nonmarine, uppermost Miocene-Pliocene Etchegoin Formation, which itself is folded on Coalinga anticline and Monocline Ridge (figs. 2 and 6) in reflection of ongoing San Andreas deformation. During this period, the Vallecitos syncline at times was topographically isolated and housed a lake, whose record is a poorly dated but likely Pliocene unnamed ostracod-bearing serpentinous mudstone that is the youngest unit folded into the syncline (Rentschler, 1985).

Big Blue Depositional Facies

The Big Blue Formation outcrop belt provides an oblique cross-sectional view of the Big Blue depositional system for about 30 km, from the edge of the protrusive

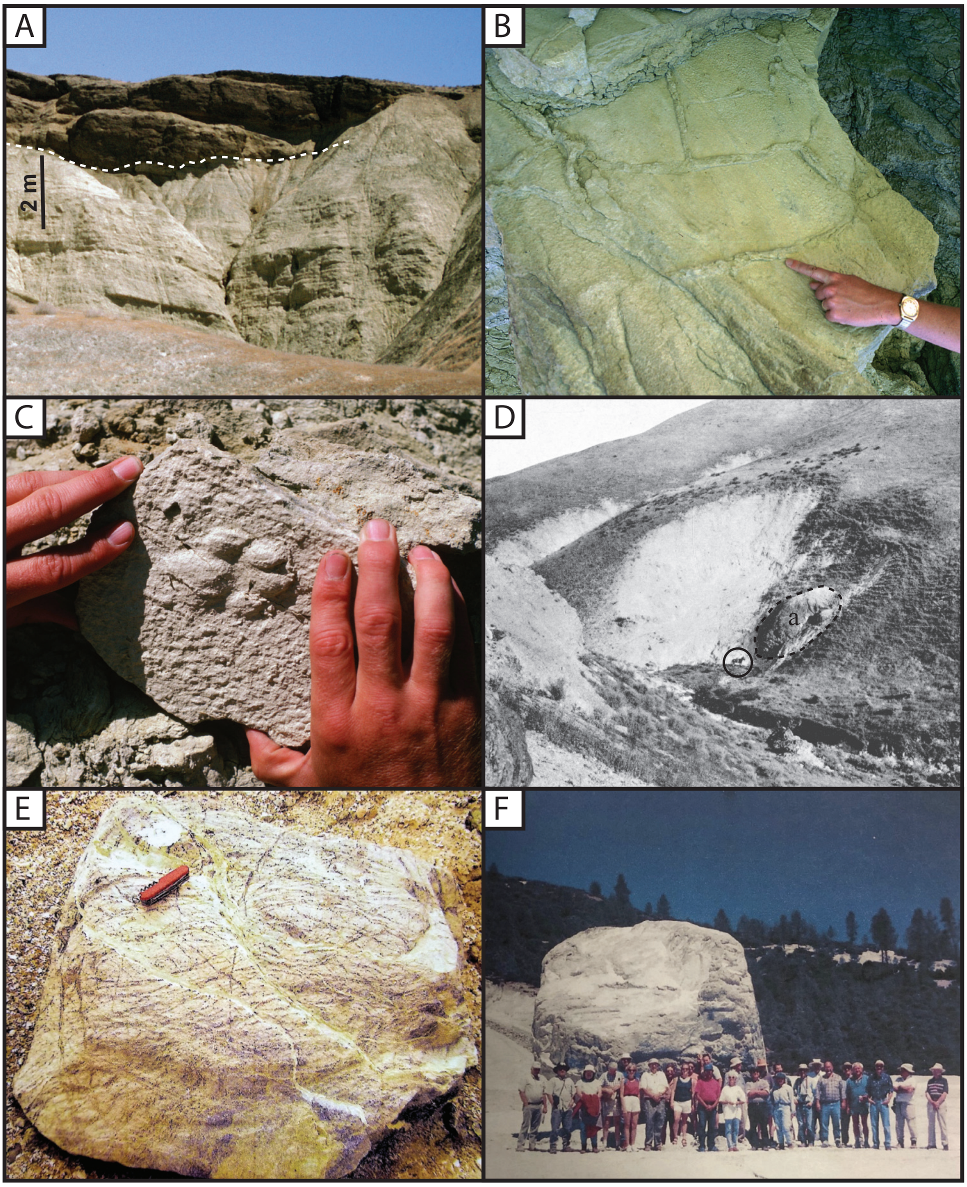

Figure 9. Outcrop photos of the New Idria serpentinite body and associated middle Miocene strata. (A) Cliff exposure of the Big Blue Formation containing lenses of conglomerate. Erosional bases of conglomerate are traced with a dashed white line. (B) Casts of polygonal desiccation cracks in serpentinous mudstone facies. (C) Cast of a canine paw trace in serpentinous mudstone facies (similar photo is shown in Bate, 1985). (D) Exposure of foliate serpentinite breccia facies of Casey and Dickinson (1976) showing a large block of antigorite serpentinite, labeled "a" just above a horse (circled), encased in flaky sheared serpentinite (from Arnold and Anderson, 1910). (E) Serpentinite block from the Joe Pit asbestos mine. The exterior surface has been gouged and rounded by abrasion within the plastic New Idria diapiric mass. The interior exhibits multiple sets of fractures due to rotation of the block during protrusion. (F) Coherent tectonic block of serpentinite exposed in the KCAC open pit asbestos mine in the southern end of the New Idria protrusion.

mass downslope through bouldery to gravelly braided stream deposits, to lower gradient stream deposits, and finally to distal muddy coastal tidal flat deposits, all comprising serpentinous detritus (figs. 8 and 9). The Big Blue Formation also extends an unknown distance to the east of the outcrop in the subsurface, where it has been reported in some petroleum exploration wells (Bate, 1985; Beery, 1988).

The Big Blue Formation comprises three principle lithofacies (Casey and Dickinson, 1976; Bate, 1985; Beery, ms, 1988): (1) foliate serpentinite breccia; (2) bedded conglomerate and breccia (3) serpentinous sandstone and claystone. The foliate serpentinite breccia lithofacies consists of flakey serpentinite with a distinct foliation, in which are set porphyroclasts of massive serpentinite featuring tectonically polished surfaces and ranging in size from centimeters to 10 meters across (fig. 9D, E, and F). This lithofacies crops out for about 3 km along Martinez Creek, where it comprises the entire Big Blue Formation and attains its greatest stratigraphic thickness at 250 m.

The proximal conglomeratic lithofacies is well developed laterally to the foliate serpentinite breccia to the north and south. The conglomeratic lithofacies consists of well-bedded gravel to cobble conglomerate organized into sheets and lenticular channel-fills (fig. 9A), interpreted as braided stream deposits by Casey and Dickinson (1976), Bate (ms, 1984, 1985) and Beery (ms, 1988). Clasts consist nearly entirely of sub-angular to subrounded serpentine, set in a serpentine-sand matrix. Casey and Dickinson (1976) reported that the conglomeratic lithofacies generally laps onto the foliate serpentinite, but locally appears to interfinger with it, indicating that the protrusive serpentine locally overrode its own detritus.

The serpentinous sandstone and claystone lithofacies interfingers laterally with the conglomeratic lithofacies, and dominates the Big Blue Formation in the northern and southern distal ends of the outcrop belt. Most sandstone beds are well laminated. The exact depositional environment of this lithofacies is uncertain. Bate (1985) recognized mud cracks, a robust shallow marine ichnofossil assemblage, and a canine pawprint in serpentinous mudstone in the southern part of the outcrop belt (fig. 9B and C), from which he inferred a tidal flat environment (fig. 8). At its southern outcrop limit near the crest of Coalinga anticline, the Big Blue Formation transitions over a distance of 2 km from 40 m of interbedded serpentinous fine conglomerate, sandstone and mudstone to less than 10 m of flakey serpentinous mudstone. The Big Blue Formation ultimately merges into the uppermost member of the quartzo-feldspathic shallow marine Temblor Formation (Bate, 1985). Serpentinous detritus did not persist in the rigors of a shallow marine environment dominated by quartz and feldspar grains (Bent, 1985), but Woodring and others (1940) noted a concentration of uvarovite and serpentine grains in the "First Zone" of the Temblor Formation, its uppermost unit, in Kettleman North Dome oilfield, some 35 km to the southeast. Bent (1985) interpreted this zone as a basinward correlation marker to the Big Blue Formation.

Geophysical and Geologic Constraints on Structure

Synthesis of the geophysical data gathered by the USGS from the 1983 Coalinga earthquake and the USGS San Andreas Fault Observatory at Depth (SAFOD) Parkfield studies provides an explanation for the New Idria structure (Rymer and Ellsworth, 1990; Wentworth and others, 1993; Hickman and Langbein, 2004; McPhee, 2004). Minor earthquakes to the south in the Kettleman Hills antiform (Guzofski and others, 2007) support the above conclusions. The surface expression of eastward thrusting seen in seismic profiles is a tectonic wedge of Franciscan mélange consisting of trench sediments and detached serpentinized abyssal peridotites, as illustrated by Wentworth and Zoback (1989, 1990). Geophysical measurements cannot distinguish between Great Valley and Franciscan ophiolites, and deeper ocean crust from the subducted Farallon plate (fig. 10). Therefore, published reconstructions usually show the basement beneath the

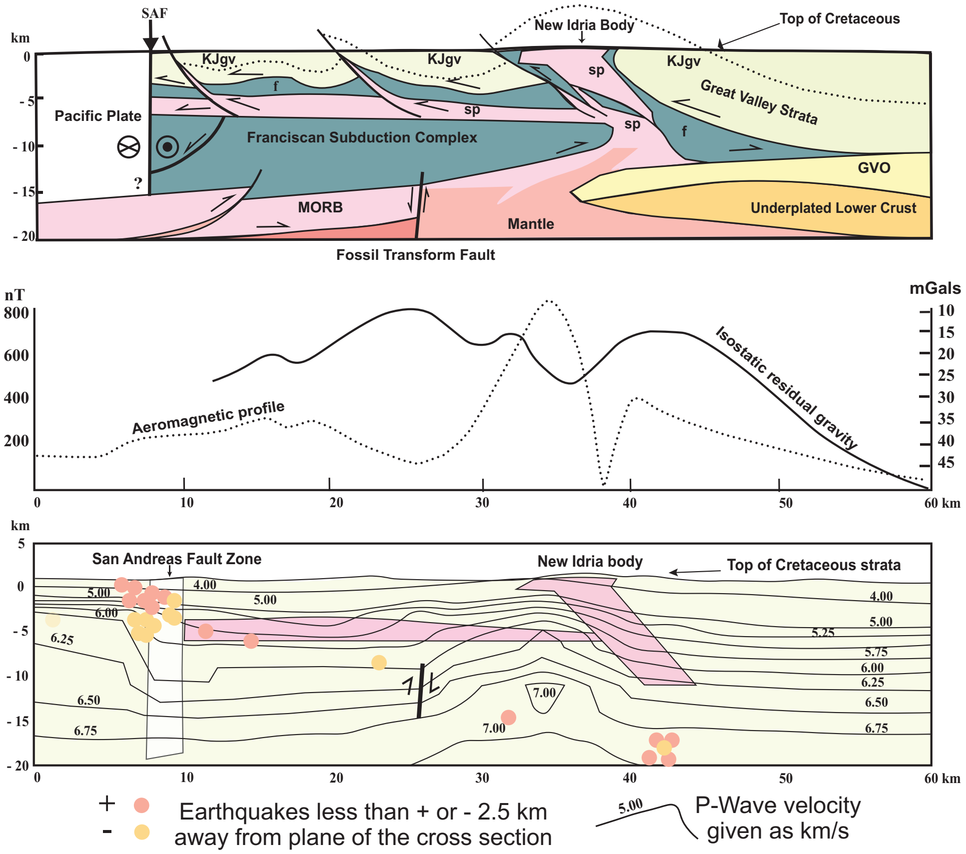

Figure 10. Geophysical cross section (bottom) and geologic interpretation (top) located on figure 2. The dome shape of the contours under the New Idria protrusion suggest upward expansion of the serpentinite due to periodic rheologic and metasomatic volume change of 15–20% minus 20 mGals of gravity. Location of the serpentinite body estimated by forward modeling (Robert Jachens, USGS, written communication, 1996). Contour values for measured P-wave velocity are given as kilometers per second. The aeromagnetic profile has increased nearly 100% due to the formation of magnetite. The locations of recent seismic events are shown as pink and yellow circles. The serpentinite protrusion shape is estimated by forward modeling of the magnetic anomolies. Dark line contours show P-wave velocities as km/s. Data taken from Wentworth and others (1992).

Coalinga antiform as a continuous monolithologic unit consisting of Great Valley basement (ophiolite) (fig. 6) (Griscom and Jachens, 1990; Namson and others, 1990; Walter, 1990; Wentworth and Zoback, 1990).

Although the Coalinga anticline had an ancestral expression well before deposition of the Big Blue Formation, extensive folding of San Joaquin basin fill was concomitant with northward propagation of the San Andreas fault, facilitated by the petrophysical contrast between igneous/metamorphic arc basement west of the San Andreas fault and sheared Franciscan Complex subduction complex basement to the east (Graham, 1987). Harding (1976) documented San Andreas-related folding adjacent to the fault in the southern and central San Joaquin Basin by late early Miocene time, coeval with passage of the Mendocino Triple Junction at that latitude (fig. 1) (Atwater and Stock, 1998). Transpressional shortening intensified across the central California Coast Ranges in latest Miocene and Pliocene, seemingly in response to a slight change in pole of rotation between the Pacific and North America plate pair

(Miller and Graham, 2018). Namson and others (1990) constructed a balanced structure section across Coalinga anticline down-plunge of the exposed New Idria serpentinite body and inferred about 11 kilometers of late Cenozoic shortening. This contraction continues to the present, judging from the 1983 Coalinga earthquake. Namson and others (1990) depicted Great Valley forearc strata as resting depositionally upon the low-pressure Coast Range Ophiolite in their cross section. By inference, the updip New Idria serpentine body should be linked to the CRO shown in their cross section (fig. 6), but the New Idria body clearly is not an ophiolite sequence, given its pervasively sheared serpentinous nature and inclusion of high-pressure/low-temperature (HP/LT) eclogitic and other exotic tectonoclasts (fig. 4) derived from depths of 40 km or more. While Namson and others (1990) disfavored a diapiric origin for the New Idria serpentine body, thrust shortening and diapirism are intrinsically linked in many salt provinces around the world (for example, Jackson and others, 1990; Harrison, 1995; Letouzey and others, 1995; Sans and Vergés, 1995; Hudec and Jackson, 2012).

The transpressional regime between the San Andreas fault and the Great Valley forearc sequence (Page and others, 1998) has produced eastward wedging of the stranded Franciscan mélange and underlying Farallon oceanic crust (Wentworth and others, 1984; fig, 6). Detached and stranded slabs of oceanic crust consisting of upper mantle abyssal peridotite within the mélange were partly serpentinized by seawater invading the new compressional regime produced by this change in plate motion (Page and Brocher, 1993). Marine water pumping into the detached abyssal peridotite as it wedged into the Franciscan mélange promoted serpentinization and diapirism. Continued transpression along the east side of the San Andreas fault to the present time has produced the New Idria serpentinite diapir (Vermeesch and others, 2006; Tsujimori and others, 2007a). The abyssal peridotite→serpentine protrusion expanded and weakened during its aseismic rheological and metasomatic transformation (Roland and others, 2010).

The rheological properties of the serpentine at the surface highly contrast with its parent, abyssal peridotite (fig. 11). A volume increase of 40 to 50% and density decrease of 24% (3.33 to 2.55 g/cc), accompanied by increasing Poisson's ratio, led to buoyancy and weakness (Escartín and others, 2001). This decrease in density and strength enabled buoyancy forces to insert the serpentinite within the Franciscan, as low-density, weak serpentinite rose laterally, lubricating blind thrust faults (Coleman, 1980a; Irwin, 1977). Earlier formed HP/LT metamorphic blocks of eclogite and blueschist in the truncated subduction zone became entrained within the serpentinite (figs. 4 and 6). Many active landslides mark the flanks of the New Idria serpentinite protrusion (fig. 4). From these, Cowan and Mansfield (1970) estimated a shear strength of 1 bar (10^6 dynes/cm^2) for the serpentinite diapir. Deposition of detrital serpentinite in Los Gatos Creek terrace deposits as young as 500 years old (Atwater and others, 1990) indicates that the New Idria serpentinite mass continues to protrude upward. It will do so as long as the tectonic transpressive regime of the San Andreas fault prevails and sub-surface serpentinization of the peridotite wedge within the Franciscan mélange continues (Reynard and others, 2007).

Wentworth and others (1993) inferred that blind thrusting during the 1983 Coalinga earthquake under the crest of the Coalinga anticline along Los Gatos Creek resulted in more than a meter of uplift. Integrating periodicity of earthquakes over a longer time period and estimating repeat times (200 to 1000 yr) for similar intensity earthquakes yields a late Holocene uplift rate of 1–2 mm/yr (Stein and King, 1984; Atwater and others, 1990). Assuming for simplicity that repeat times for seismic events have remained constant for the last 20 Myr, the New Idria/Coalinga anticline area could have undergone more than 20,000 to 100,000 seismic events related to

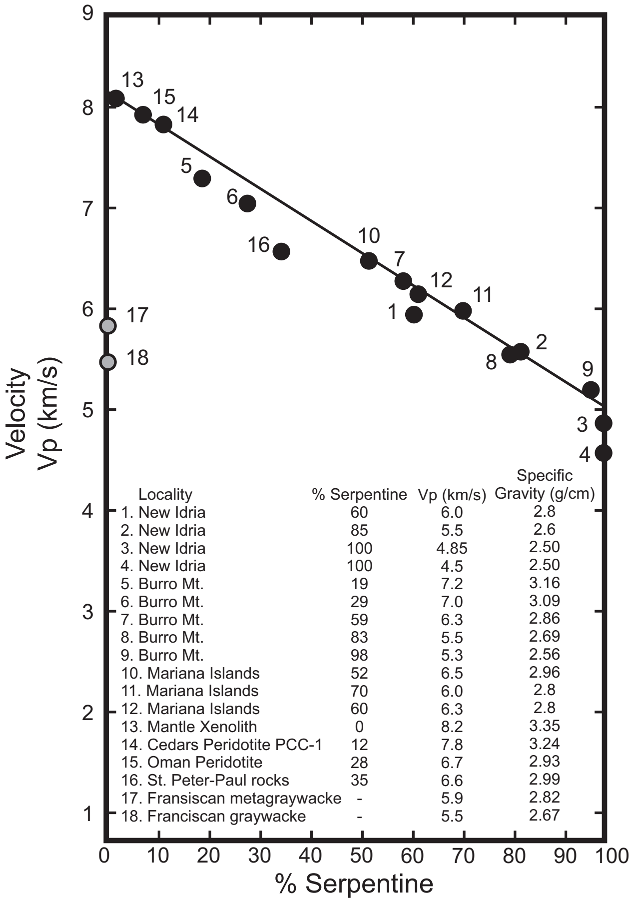

Locality	% Serpentine	Vp (km/s)	Specific Gravity (g/cm)
1. New Idria	60	6.0	2.8
2. New Idria	85	5.5	2.6
3. New Idria	100	4.85	2.50
4. New Idria	100	4.5	2.50
5. Burro Mt.	19	7.2	3.16
6. Burro Mt.	29	7.0	3.09
7. Burro Mt.	59	6.3	2.86
8. Burro Mt.	83	5.5	2.69
9. Burro Mt.	98	5.3	2.56
10. Mariana Islands	52	6.5	2.96
11. Mariana Islands	70	6.0	2.8
12. Mariana Islands	60	6.3	2.8
13. Mantle Xenolith	0	8.2	3.35
14. Cedars Peridotite PCC-1	12	7.8	3.24
15. Oman Peridotite	28	6.7	2.93
16. St. Peter-Paul rocks	35	6.6	2.99
17. Fransiscan metagraywacke	-	5.9	2.82
18. Franciscan graywacke	-	5.5	2.67

Figure 11. Selected abyssal peridotites in various stages of serpentinization showing a linear relationship with changes in their rheological properties during long-term tectonic deformation. Seismic velocity is shown as compressional wave velocity Vp km/sec obtained by geophysical field and/or laboratory measurements. Vp is plotted against percentage of serpentine in the metasomatized peridotites. Serpentine percentage in the peridotite also can be estimated by petrographic methods, using specific gravity or by measuring (H_2O) loss on ignition (LOI). St Peter's and St Paul's abyssal peridotite (sample 16) protruding within transform faults transecting the Mid-Atlantic Ridge (Melson and others, 1972; Bonatti, 1976). Samples 17 and 18 weight by (LOI) during wet chemical analysis (Escartín and others, 2001; Carlson and Miller, 2003; Mevel, 2003). Surface samples 1–4 are from New Idria serpentine body and illustrate the great range in degree of serpentinization. Seismic traverse across the body reveals 100% serpentine at the surface, 58% at 6 km depth and 42% at 15 km depth (Robert Jachens, USGS, written communication, 1996). Samples 5–9 from Burro Mountain peridotite–serpentine protrusion 85 km west of New Idria with a core of peridotite that is 19% serpentine and a peripheral zone of 98% serpentine using LOI (Coleman and Keith, 1971; Loney and others, 1971). Samples 10,11,12 from the Mariana Arc Islands are from serpentine protrusions (mud volcanos) that contain xenoliths of peridotite-serpentine that are 70 to 52% serpentine with a seismic velocity 5.2 to 7.0 Vp km/sec (Ballotti and others, 1992). Sample 13 is an unaltered peridotite xenolith from Jabal Turf Quaternary alkali basalt, Saudi Arabia, estimated to have originated at depth of 25 km, as a good example of a dry abyssal peridotites that formed within an oceanic spreading center (Ghent and others, 1980). Sample 14, Cedars abyssal peridotite, northern California (PCC-1 USGS standard rock sample), has been analyzed many times in different laboratories (Flanagan, 1969; Blake and others, 2012) and now is used as typical of depleted abyssal peridotite of the upper mantle. Sample 15 is abyssal peridotite from the Semail ophiolite in Oman that has been analyzed by numerous studies (Boudier and Coleman, 1981; Christensen and Smewing, 1981). Sample 17 and 18 are greywackes within the Franciscan mélange where the meta-greywackes have distinctly higher density and Vp velocities than the unaltered sediments. These different rheologies overlap those of serpentinized peridotite, making it difficult to distinguish the lithologies within the Franciscan mélanges using only geophysical methods (Brocher, 2005).

continued blind thrusting, enabling the diapiric rise of the serpentinite protrusion (Atwater and others, 1990; Stein and King, 1984). Each of these seismic and/or aseismic events would introduce additional water into the system to sustain the peridotite to serpentine metasomatism and expansion. Similarly, Berry (1973) suggested that the high fluid pressure present today proximal to the Coast Ranges (for example, Yerkes and others, 1990; Johnson and McEvilly, 1995) may result from aseismic creep where serpentinite is present along the San Andreas, Hayward, and Calaveras faults (Moore and Rymer, 2007; Moore and Lockner, 2013). Forty kilometers north of the New Idria serpentine body where the San Andreas and Calaveras faults converge, geophysical modeling reveals tabular folded serpentinite bodies detaching and ascending on a décollement within Franciscan mélange (Watt and others, 2014). Modeling of the New Idria magnetic anomaly and seismic velocities suggests a volume of 200 to 250 km^3 of serpentinite remains to be protruded in the future (fig. 1).

EVOLUTION AND UPLIFT OF THE NEW IDRIA DIAPIR

The deformational history of the New Idria serpentinized peridotite is critical to understanding its formation and protrusion within the Franciscan forearc mélange (ten Brink and others, 1999). Field geophysical measurements for gravity, magnetic, and GPS have been made, as well as laboratory studies of density, seismic velocities, magnetic properties, and bulk rock + mineral chemical and trace element analysis (Hickman and Langbein, 2004). Large-scale geologic mapping has established stratigraphic and structural relationships (Coleman, 1996; Tsujimori and others, 2007a). Combined geologic and new GPS measurements along the San Andreas fault reveal transpressional folding of the Franciscan mélange and Great Valley strata (Titus and others, 2011). This regional stress produced numerous plastic protrusions of serpentine on the eastern side of the San Andreas fault from Table Mountain to New Idria and to the San Francisco Bay region (fig. 1) (Dickinson, 1966; Wentworth and Zoback, 1989; McPhee and others, 2004; Blakely and others, 2005). The transpression which developed after the Mendocino Triple Junction passed the latitude of New Idria in middle Miocene time produced east-directed blind thrusting of serpentinite into Franciscan mélange. Using a decade of GPS-In SAR satellite measurements along the 240 km creeping segment San Andreas fault between San Juan Bautista and Parkfield, Ryder and Bürgmann (2008) established a horizontal surface aseismic creep rate of up to ~31 mm/yr and a deep-slip rate of ~33 mm/yr. They also determined a relative uplift rate of 7 mm/yr, almost twice the rate deduced from long-term geologic estimates of 4 mm/yr attributable to the diapiric rise of the New Idria serpentinite and non-tectonic signals, such as agriculture groundwater withdrawal and oil production.

Significantly, recorded earthquake epicenters are sparse within the New Idria serpentinite dome and other smaller diapiric bodies along this 250 km creeping segment of the San Andreas fault (Titus and others, 2011). The lack of seismic activity within these protrusions suggests that serpentinite continues its expansion by a combination of aseismic tectonic transpressive forces produced by the San Andreas fault (Platt and others, 2018), along with a weak plastic serpentinite mass modulated by the activity of H_2O (Moore and Rymer, 2007). Bonnin and others (2010) used SKS (shear wave splitting) within the crust and mantle (asthenosphere) along the San Andreas fault in central coastal California as far south as the New Idria diapir to distinguish a deformational boundary that formed serpentinite at the level of the former Moho. Weak gravity measurements over the New Idria diapir support the idea that mobile serpentinite is an integral part of San Andreas fault deformation.

The geodynamic rates of serpentinization over time are difficult to estimate. The Coast Ranges of California are rising at an average rate of 2 to 3 mm/yr (Page and others, 1998) and the New Idria, Burro Mountain, and Mount Diablo serpentine protrusions have measured rates of 4 to 7 mm/yr (Coleman, 1996; Tsujimori and others, 2007a; Ryder and Bürgmann, 2008). The exhumation rate of a serpentinite diapir would be a function of its degree of serpentinization, shape of the body, and especially, its size: larger masses for a specific degree of serpentinization would have body forces greater than the frictional resistance of the country rock walls and would ascend faster than smaller diapirs. However, this observation is not informative about the rate of serpentinization, which is controlled by P, T, and composition of the aqueous fluid, as well as the spatial parameters.

SYNTHESIS AND DISCUSSION

The protolith of the New Idria serpentinite protrusion has been generally interpreted as an abyssal peridotite restite produced by basaltic melt extracted beneath an oceanic spreading center (Coleman, 1996). However, it should be noted that recent comparison of bulk-rock geochemistry of New Idria serpentinites to global geochemical compilation has shown, in part, greater geochemical similarities to depleted mantle wedge rather than highly variable abyssal serpentinites (Lazar and others, 2021). Reflecting wholesale serpentinization, only minor amounts of the original peridotite now exist within the New Idria diapir. The serpentinite dome is in fault contact with surrounding marine Mesozoic and Cenozoic sedimentary rocks (Dibblee, 1972, 2007) (fig. 2). These flanking rocks include Franciscan mélange of Jurassic-Cretaceous age, Upper Cretaceous Panoche and Moreno formations of the Great Valley forearc basin fill, and overlying Cenozoic sequences of marine sandstone and shale (Coleman, 1986) (fig. 3).

The basement for the west side of the Mesozoic Great Valley forearc sequence is considered to be oceanic crust (Orme and Graham, 2018) that formed as part of an intra-oceanic arc system in Late Jurassic time, 161 to 169 Ma (Hopson and others, 1981; Coleman, 1986; Robertson, 1989). Cenozoic marine strata as young as Pliocene age unconformably overlie the folded Franciscan mélange and Mesozoic forearc basin strata of the Great Valley Group (Dibblee, 1971; Nilsen and Dibblee, 1979; Mattinson and Echeverria, 1980). The contact of the serpentinite body with the surrounding sediments is marked by high angle faults and shear zones that indicate upward differential movement of the serpentinite body relative to the surrounding mélange and sedimentary strata (Coleman, 1980a, 1980b, 1996) (fig. 2). The northeastern contact along the New Idria serpentinite with overlying strata is a thrust, as the subjacent Mesozoic and Cenozoic sediments are overturned to the east by the serpentinite protrusion (Eckel and Myers, 1946; Coleman, 1957). Wentworth and others (1984), Jachens and others (1995), and McPhee and others (2004) used seismic refraction data to infer that extensive structural wedging of Franciscan mélange beneath the Great Valley forearc strata and underlying oceanic crust took place in the Miocene, although stratigraphic evidence (Harding, 1976; McGuire, 1988a,b; Mitchell and others, 2010; Sharman and others, 2017), indicates that an ancestral version of the Diablo Range and specifically Coalinga anticline, existed as early as the Maastrichtian.

When the MTJ initiated *ca.* 28 Ma and migrated past the latitude of New Idria near the end of the middle Miocene (*ca.* 12–14 Ma), based on outcrop patterns of dated volcanics (for example Dickinson, 1997) (fig. 1) and plate reconstructions of Stock and Molnar (1988), the crust-cutting San Andreas transform fault allowed seawater to invade the upper mantle. Serpentine began to replace abyssal peridotite as detachment and wedging produced fractures that allowed marine water to initiate a slow metasomatism of the abyssal peridotite. The result was a profound decrease in density and strength, and an increase in volume. Accordingly, a large fragment of now-buoyant abyssal peridotite derived from the previously subducting Kula plate (Warren, 2016) disengaged from the downgoing oceanic lithosphere, and ascended into the Franciscan mélange wedged under the Great Valley forearc sequence (Wentworth and others, 1984; fig. 4).

The regional fault that marks the present-day contact between the Great Valley forearc sequence and the Franciscan mélange is called the Coast Range thrust (Bailey and others, 1964, Graymer and others, 2014). This tectonic contact was first thought to represent the preserved trace of the Mesozoic subduction zone (Ernst, 1970), but the seismic evidence produced by Wentworth and others (1984) and Jachens and others (1995) does not support this idea in the New Idria area. The faults marking the boundary between the New Idria serpentinite protrusion and the surrounding Franciscan mélange represent a detached segment of the Coast Rage thrust (figs. 2 and 6). Wedging of the detached Franciscan mélange under the Great Valley forearc sediments further elevated the ancestral Diablo Range, while weak and expanding serpentinite rose buoyantly within thrust sheets and into the pre-existent Coalinga anticline (fig. 6). San Andreas fault tectonics produced northeast-directed transpressive folding (Titus and others, 2007; Dickinson and Snyder, 1979; Graham and Williams, 1985; Rentschler and Bloch, 1988; Namson and Davis, 1988; Graham and others, 1989; Tsujimori and others, 2007a; Miller and Graham, 2018) that, combined with the rheology of a weak, plastic, and expanding serpentinite-peridotite mass, permitted upward protrusion into the pre-existent Coalinga anticline at an estimated 5 cm/yr.

The New Idria serpentinite body breached the surface in middle Miocene time, as marked by local concentrations of serpentine detritus in the Temblor Formation (fig. 3) and much more expansive serpentine deposits in the Big Blue Formation (figs. 2 and 3), which developed as an alluvial apron off the eastern flank of the New Idria uplift (Casey and Dickinson, 1976; Bate, ms, 1984, 1985; Carlson and others, 1984; Beery, ms, 1988) (fig. 3). Thereafter, denudation of this spectacular protrusion left a continuous record of detrital serpentine in the San Joaquin Basin and Vallecitos syncline, as demonstrated by serpentinous mud, sand and pebbles within the Etchegoin (5.5–4.5 Ma), San Joaquin (4.5–2.5 Ma) and Tulare (2.5–0.6 Ma) formations, as well as in modern stream deposits (per age assignments of Scheirer and Magoon, 2006).

A small amount of alkali basalt magma differentiated to syenite and intruded the southern part of the New Idria diapir (figs. 3 and 4). During the middle Miocene (~12 Ma), it enhanced metasomatic alteration in restricted zones within the serpentinite and tectonic inclusions (Coleman, 1957) (fig. 4). These metasomatic alterations produced the California State gem benitoite ($BaTiSi_3O_9$), dated at *ca.* 12 Ma (Laurs and others, 1997; Obradovich and others, 2000). Continued upward diapiric movement of the New Idria serpentinite body to the present has elevated and exposed tectonic inclusions that preserve a HP/LT blueschist-eclogite metamorphic history. Fission track dating of detrital apatite from Great Valley forearc sediments nearest to their contact with the New Idria serpentinite diapir have an apparent age of 13 Ma (Vermeesch and others, 2006). These fission track ages coincide with the passage of the Mendocino Triple Junction, and the initial protrusion of the New Idria serpentinite, as well as the igneous intrusion of syenite, alkali basalt, and metasomatic formation of the gem minerals benitoite and neptunite within the protrusion.

Offset depositional contacts that developed during exhumation of the New Idria serpentinite mélange indicate a possible vertical uplift rate of ~4–5 mm/yr, nearly four times the average rate for the California Coast Range of 1 mm/yr (Page and others, 1998). Further evidence of this uplift rate is given by a small patch of Pliocene sediments deposited upon the north end of the serpentine body (figs. 2 and 4). These rocks are correlated with the youngest sediments deposited in the Vallecitos syncline at ~2–5 Ma (Rentschler, 1985). The vertical displacement between the trough of the syncline and the small patch of sediments on the crest of the New Idria serpentinite dome is 850 meters, supporting the estimate for the Pliocene uplift rate of ~5 mm/yr (Coleman, 1996).

CONCLUSION

The classification of isolated peridotite bodies as Alpine-type ultramafic igneous intrusions gave way to an interpretation that these bodies were detached fragments of upper mantle peridotite emplaced as a consequence of tectonic and metasomatic processes (Coleman, 1980b, 1996). Geochemical and rheological studies indicate that many such serpentinite bodies in western California were plastic mobile protrusions driven by continuous expansion during metasomatism attending San Andreas transform evolution (Tsujimori and others, 2007a). Protrusion is initiated by a volume increase as small as 12%, reducing density and increasing Poisson's ratio, thereby facilitating the weak and plastic serpentinite-peridotite mass to rise along blind thrust faults into brittle sedimentary cover strata.

The New Idria protrusion first breached the surface 14–18 Ma and was widely exposed by 14 Ma, reflecting passage of the migrating Mendocino Triple Junction. As the Mendocino Triple Junction continued its northward migration past the latitude of San Francisco Bay, and the San Andreas fault evolved in its wake, transform faulting and fracturing allowed seawater to penetrate into the upper mantle abyssal peridotite within the fault zone; this fluid initiated serpentinization (metasomatism). Transpressional tectonic forces developed along the San Andreas fault between the Pacific and North American plates mobilized weak, plastic, buoyant serpentinite bodies that form upward bulbous detachments that gradually protruded to the surface as elongate domes. Approximately 11 km of E-W horizontal shortening on the east side of the San Andreas fault at the latitude of Coalinga (Namson and others, 1990) reflects transpression integral to the story of New Idria's diapiric evolution.

ACKNOWEDGMENTS

We dedicate this paper to our co-author, friend and mentor, the late Robert G. Coleman. The authors thank W. Gary Ernst for reviewing an early version of this paper and Sarah Titus for providing a thoughtful journal review. Completion of revisions of this manuscript was partially funded by the U.S. Geological Survey Energy Resource Program. Any use of trade, firm, or product names is for descriptive purposes only and does not imply endorsement by the U.S. Government.

REFERENCES

Adegoke, G. S., 1969, Stratigraphy and paleontology of the marine Neogene formations of the Coalinga region, California: University of California Publications in Geological Sciences, v. 80, 269 p.

Amiguet, E., Reynard, B., Caracas, R., Van de Moortèle, B., Hilairet, N., and Wang, Y., 2012, Creep of phyllosilicates at the onset of plate tectonics: Earth and Planetary Science Letters, v. 345–348, p. 142–150, https://doi.org/10.1016/j.epsl.2012.06.033

Anderson, J. Q., 1952, Coalinga oil fields, in Guidebook Field Trip Routes, Oil Fields, Geology: American Association of Petroleum Geologists-Society of Economic Paleontologists and Mineralogists-Society of Exploration Geophysicists Annual Meeting, p. 177–188.

Anderson, K. S., 1996, The Paleogene Cantua Sandstone, southern Diablo Range, California: Facies architecture of a sand-rich, structural controlled, deep-sea depositional system, *in* Abbott, P. L., and Cooper, J. D., editors, Field Conference Guide 1996: The Pacific Section American Association of Petroleum Geologists, v. 73, p. 5–18, https://doi.org/10.32375/1996-GB73.2

Anderson, R., and Pack, R. W., 1915, Geology and oil resources of the west border of the San Joaquin Valley north of Coalinga, California: United States Geological Survey Bulletin, v. 603, 220 p.

Andreani, M., Mével, C., Boullier, A.-M., and Escartín, J., 2007, Dynamic control on serpentine crystallization in veins; Constraints on hydration processes in oceanic peridotites: Geochemistry, Geophysics, Geochemistry, v. 8, n. 2, Q02012, https://doi.org/10.1029/2006GC001373

Arnold, R., and Anderson, R., 1910, Geology and oil resources of the Coalinga district, California: United States Geological Survey Bulletin, v. 398, 354 p.

Atwater, B. F., Trumm, D. A., Tinsley, J. C. III, Stein, R. S., Tucker, A. B., Donahue, D. J., Jull, A. J. T., and Payen, L. A., 1990, Alluvial Plains and Earthquake Recurrence at the Coalinga Anticline, *in* Rymer, M. J., and Ellsworth, W. L., editors, The Coalinga, California, Earthquake of May 2, 1983: United States Geological Survey Professional Paper, 1487, p. 273–298.

Atwater, T., 1970, Implications of plate tectonics for the Cenozoic tectonic evolution of western North America: Geological Society of America Bulletin, v. 81, n. 12, p. 3513–3536, https://doi.org/10.1130/0016-7606(1970)81[3513:IOPTFT]2.0.CO;2

Atwater, T., 1989, Plate tectonic history of the Northeast Pacific and western North America, *in* Hussong, D. M., and Decker, R. W., editors, The Geology of North America—The Eastern Pacific Ocean and Hawaii: Boulder, Colorado, Geological Society of America, v. N, p. 21–72, https://doi.org/10.1130/DNAG-GNA-N.21

Atwater, T., and Molnar, P., 1973, Relative motion of the Pacific and North American plates deduced from sea-floor spreading in the Atlantic, Indian, and South Pacific oceans, *in* Kovach, R. L., and Nur, A., editors, Proceedings of the Conference on Tectonic Problems of the San Andreas Fault System: Stanford University Publications in Geological Science, v. 12, p. 136–148.

Atwater, T., and Stock, J., 1998, Pacific-North America plate tectonics of the Neogene southwestern United States: an update: International Geological Review, v. 40, n. 5, p. 375–402, https://doi.org/10.1080/00206819809465216

Bach, W., Jöns, N., and Klein, F., 2012, Metasomatism within the ocean crust: *in* Harlov, D. E., and Austrheim, H., editors, Metasomatism and the Chemical Transformation of Rock, Lecture notes in Earth Systems, Chapter 5: Springer, Berlin Heidelberg, p. 253–288, https://doi.org/10.1007/978-3-642-28394-9_8

Bailey, E. H., Irwin, P. I., and Jones, D. L., 1964, Franciscan and related rocks, and their significance in the geology of western California: California Division of Mines and Geology Bulletin, v. 183, p. 1–177.

Ballotti, D. M., Christensen, N. I., and Becker, K., 1992, Seismic properties of Serpentinized Peridotite from the Mariana Forearc: Proceedings Ocean Drilling Program Initial scientific Results, v. 125, p.581–584, https://doi.org/10.2973/odp.proc.sr.125.161.1992

Barnes, I., Rapp, J. B., O'Neil, J. R., Sheppard, R. A., and Gude, A. J. III, 1972, Metamorphic assemblages and the direction of flow of metamorphic fluids in four instances of serpentinization: Contributions to Mineralogy and Petrology, v. 35, p. 263–276, https://doi.org/10.1007/BF00371220

Bate, M. A., ms, 1984, Temblor and Big Blue formations; interpretation of depositional environment sequence on Coalinga Anticline, Fresno County, California: Master's thesis, Stanford University, Stanford, 123 p.

Bate, M. A., 1985, Depositional sequence of Temblor and Big Blue Formations, Coalinga Anticline, California, *in* Graham, S. A., editor, Geology of the Temblor Formation, western San Joaquin basin, California: Pacific Section, Society Economic Paleontologists and Mineralogists, v. 44, p. 69–86.

Bayrakci, G., Minshull, T. A., Sawyer, D. S., Reston, T. J., Klaeschen, D., Papenberg, C., Ranero, C., Bull, J. M., Davy, R. G., Shillington, D. J., Perez-Gussinye, M., and Morgan, J. K., 2016, Fault-controlled hydration of the upper mantle during continental rifting: Nature Geoscience, v. 9, p. 384–388, https://doi.org/10.1038/ngeo2671

Beery, J., ms, 1988, Depositional history and paleo-environments of the lower and middle Miocene Temblor Formation, northern San Joaquin basin, California: Master's thesis, Stanford University, Stanford, 132 p.

Bent, J., 1985, Provenance of upper Oligocene-middle Miocene sandstones of the San Joaquin basin, California, *in* Graham, S. A., editor, 1985, Geology of the Temblor Formation, western San Joaquin basin, California: Pacific Section, Society Economic Paleontologists and Mineralogists, v. 44, p. 97–120.

Berry, F. A. F., 1973, High fluid potentials in California Coast Ranges and their tectonic significance: American Association of Petroleum Geologists Bulletin, v. 57, n. 7, p. 1219–1249, https://doi.org/10.1306/83D90E8A-16C7-11D7-8645000102C1865D

Bezacier, L., Reynard, B., Cardon, H., Montagnac, G., and Bass, J. D., 2013, High-pressure elasticity of serpentine and seismic properties of the hydrated mantle wedge: Journal of Geophysical Research: Solid Earth, v. 118, n. 2, p. 527–535, https://doi.org/10.1002/jgrb.50076

Blake , M. C., Jr., Bailey, E. H., and Wentworth, C. M., 2012, The Cedars ultramafic mass, Sonoma County: U.S. Geological Survey, Open-File Report, 2012–1164, 13 p., https://doi.org/10.3133/ofr20121164

Blakely, R. J., Brocher, T. M., and Wells, R. E., 2005, Subduction-zone magnetic anomalies implications for hydrated forearc mantle: Geology, v. 33, n. 6, 445–448, https://doi.org/10.1130/G21447.1

Bloch, R. B., von Huene, R., Hart, P. E., and Wentworth, C. M., 1993, Style and magnitude of tectonic shortening normal to the San Andreas fault across Pyramid Hills and Kettleman Hills South Dome, California: Geological Society of America Bulletin, v. 105, n. 4, p. 464–478, https://doi.org/10.1130/0016-7606(1993)105<0464:SAMOTS>2.3.CO;2

Bonatti, E., 1976, Serpentinite protrusions in the oceanic crust: Earth and Planetary Science Letters, v. 32, n. 2, p. 107-113, https://doi.org/10.1016/0012-821X(76)90048-0

Bonnin, M., Barruol, G., and Bokelmann, G. H. R., 2010, Upper mantle deformation beneath the north American-Pacific plate boundary in California from SKS splitting: Journal of Geophysical Research: Solid Earth, v. 115, n. B4, https://doi.org/10.1029/2009JB006438

Boudier, F., and Coleman, R. G., 1981, Cross section through the peridotite in the Semail ophiolite, southeastern Oman Mountains: Journal of Geophysical Research: Solid Earth, v. 86, p. 2573–2592, https://doi.org/10.1029/JB086iB04p02573

Bramlette, M. N., 1946, The Monterey Formation of California and its origin of its siliceous rocks: U.S. Geological Survey Professional Paper, v. 212, p.1–60, https://doi.org/10.3133/pp212

Brocher, T., 2005, Compressional and shear wave velocity versus depth in the San Francisco Bay Area, California: Rules for USGS Bay Area Velocity Model 05.0.0: US Geological Survey, Open File Report 2005-1317, https://doi.org/10.3133/ofr20051317

Carlson, C. L., Bate, M. A., Casey, T. A. L., and Dickinson, W. R., 1984, Depositional facies of sedimentary serpentine: Selected Examples from the Coast Ranges, California: Society of Economic Paleontologists and Mineralogists Field Trip Guidebook No. 3, 1984 Midyear Meeting, San Jose, California, p. 73–101.

Carlson, R. L., and Miller, D.J., 2003, Mantle wedge water contents estimated from seismic velocities in partially serpentinized peridotites, Geophysical Research Letters, v. 50, no. 5, https://doi.org/10.1029/2002GL016600

Casey, T. A., 1984, Sedimentary serpentinite of the Miocene Big Blue Formation near Cantua Creek: Society of Economic Paleontologists and Mineralogists Guidebook, v. 3, p. 92–97.

Casey, T. A., and Dickinson, W. R., 1976, Sedimentary serpentinite of the Miocene Big Blue Formation near Cantua Creek, California, *in* Fritsche, A. E., Ter Best, H. J., and Wornardt, W. W., editors, The Neogene Symposium; Selected Technical Papers on Paleontology, Sedimentology, Petrology, Tectonics and Geologic History of the Pacific Coast of North America: Pacific Section, Society of Economic Paleontologists and Mineralogists, p. 65–74.

Christensen, N. I., 2004, Serpentinites, peridotites, and seismology: International Geology Review, v. 46, n. 9, p. 795–816, https://doi.org/10.2747/0020-6814.46.9.795

Christensen, N. I., and Smewing, J. D., 1981, Geology and seismic structure of the northern section of the Oman ophiolite: Journal of Geophysical Research: Solid Earth, v. 86, n. B4, p. 2545–2555, https://doi.org/10.1029/JB086iB04p02545

Coleman, R. G., 1957, Mineralogy and petrology of the New Idria district, California: PhD thesis, Stanford University, Stanford, 165 p.

Coleman, R. G., 1961, Jadeite deposits of the Clear Creek area, New Idria district, San Benito County, California: Journal of Petrology, v. 2, n. 2, p. 209–247, https://doi.org/10.1093/petrology/2.2.209

Coleman, R. G., 1971, Petrologic and geophysical nature of serpentinites: Geological Society of America Bulletin, v. 82, n. 4, p. 897–918, https://doi.org/10.1130/0016-7606(1971)82[897:PAGNOS]2.0.CO;2

Coleman, R. G., 1980a, Tectonic inclusions in serpentinites: Archives des Sciences de Geneve, v. 33, p. 89–102.

Coleman, R. G., 1980b, Ophiolite tectonics and metamorphism: Colloques Internatilonaux du CNRS No. 272, Orogenic mafic-ultramafic association, p.167–184.

Coleman, R. G., 1986, Ophiolites and accretion of the North American Cordillera: Bulletin de la Société Géologique de France, v. 2, n. 6, p. 961–968, https://doi.org/10.2113/gssgfbull.II.6.961

Coleman, R. G., 1996, New Idria serpentinite: A land management dilemma: Environmental & Engineering Geoscience, v. 2, n. 1, p. 9–22, https://doi.org/10.2113/gseegeosci.II.1.9

Coleman, R. G., and Keith, T. E., 1971, A chemical study of serpentinization – Burro Mountain, California: Journal of Petrology, v. 12, n. 2, p. 311–328, https://doi.org/10.1093/petrology/12.2.311

Coleman, R. G., and Lanphere, M. A., 1971, Distribution and age of high-grade blueschists associated eclogites, and amphibolites from Oregon and California: Geological Society of America Bulletin, v. 82, n. 9, p. 2397–2412, https://doi.org/10.1130/0016-7606(1971)82[2397:DAAOHB]2.0.CO;2

Cooley, S. A., 1985, Depositional environments of the lower and middle Miocene Temblor Formation of Reef Ridge, Fresno and Kings Counties, California *in* Graham, S. A., editor, Geology of the Temblor Formation, western San Joaquin basin, California: Pacific Section, Society Economic Paleontologists and Mineralogists, v. 44, p. 35–52.

Cowan, D. S., and Mansfield, C. F., 1970, Serpentinite flows on Joaquin Ridge, Southern Coast Ranges, California: Geological Society of America Bulletin, v. 81, n. 9, p. 2615–2628, https://doi.org/10.1130/0016-7606(1970)81[2615:SFOJRS]2.0.CO;2

Dibblee, T. W. Jr., 1971, Geologic maps of seventeen 15-minute quadrangles (1:62,500) along the San Andreas fault in the vicinity of King City, Coalinga, Panoche Valley, and Paso Robles, California, with index map: U.S. Geological Survey Open-File Report, v. 71-0087, 17 sheets, scale 1:62,500, https://doi.org/10.3133/ofr7187

Dibblee, T. W. Jr., 1972, Preliminary geologic map of the San Jose East quadrangle, Santa Clara County, California: U. S. Geological Survey Open File Report, v. 72–92, scale 1:24,000, https://doi.org/10.3133/ofr7292

Dibblee, T. W. Jr., 2007, Geologic map of the Idria Quadrangle: Santa Barbara Museum of Natural History, Santa Barbara, California: Scale 1:24,000.

Dibblee, T. W. Jr., Graham, S. E., Mahoney, T. M., Blissenbach, J. L., Marinant, J. J., and Wentworth, C. M., 1999, Regional geological map of San Andreas and related faults in Carrizo Plain, Temblor, Caliente, and La Panza Ranges and vicinity, California: A digital database, U.S. Geological Survey Open File Report, v. 99–14, https://doi.org/10.3133/ofr9914

Dickinson, W. R., 1966, Table Mountain serpentine extrusion in California Coast Ranges: Geological Society of America Bulletin, v. 77, n. 5, p. 451–472, https://doi.org/10.1130/0016-7606(1966)77[451:TMSEIC]2.0.CO;2

Dickinson, W. R., 1997, Overview: Tectonic implciations of Cenozoic volcanism in coastal California: Geological Society of America Bulletin, v. 109, n. 8, p.936–954, https://doi.org/10.1130/0016-7606(1997)109<0936:OTIOCV>2.3.CO;2

Dickinson, W. R., and Snyder, W. S., 1979, Geometry of triple junctions related to San Andreas transform: Journal of Geophysical Research: Solid Earth, v. 84, n. B2, p. 561–572, https://doi.org/10.1029/JB084iB02p00561

Eckel, E. B., and Myers, W. B., 1946, Quicksilver deposits of the New Idria district, San Benito and Fresno Counties, California: California Journal of Mines and Geology, v. 42, n. 2, p. 81–124.

Ernst, W. G., 1970, Tectonic contact between the Franciscan Mélange and the Great Valley Sequence, Crustal expression of a Late Mesozoic Benioff zone: Journal of Geophysical Research, v. 75, n. 5, p. 886–901, https://doi.org/10.1029/JB075i005p00886

Escartín, J., Hirth, G., and Evans, B., 2001, Strength of slightly serpentinized peridotites: Implications for the tectonics of oceanic lithosphere: Geology, v. 29, n. 11, p.1023–1026, https://doi.org/10.1130/0091-7613(2001)029<1023:SOSSPI>2.0.CO;2

Evans, B. W., Hattori, K., and Barronet, A., 2013, Serpentinite: what, why, and where?: Elements, v. 9, n. 2, p. 99–106, https://doi.org/10.2113/gselements.9.2.99

Flanagan, F. J., 1969, U.S. Geol. Survey Standards, II. First compilation of data for the new U.S.G.S. rocks: Geochimica Cosmochimica Acta, v. 33, n. 1, p. 81–120, https://doi.org/10.1016/0016-7037(69)90094-5

Furlong, K. P., and Schwartz, S. Y., 2004, Influence of the Mendocino triple junction on the tectonics of Coastal California: Annual Reviews of Earth and Planetary Science, v. 32, p. 405–433, https://doi.org/10.1146/annurev.earth.32.101802.120252

Fyfe, W. S., and Lonsdale, P., 1981, Ocean floor hydrothermal activity, *in* Emiliani, C., editor, The Oceanic Lithosphere: New York, Wiley, p. 589–638.

Germanovich, L. N., Gene, G., Lowell, R. P., and Rona, P. A., 2012, Deformation and surface uplift associated with serpentinization at mid-ocean ridges and subduction zones: Journal of Geophysical Research: Solid Earth, v. 117, n. B7, B07103, https://doi.org/10.1029/2012JB009372

Gerya, T. V., Stöchert, B., and Perchuk; A. , I., 2002, Exhumation of high-pressure metamorphic rocks in a subduction channel: A numerical simulation: Tectonics, v. 21, n. 6, p. 6-1–6-19, https://doi.org/10.1029/2002TC001406

Ghent, E. D., and Coleman, R. G., 1973, Eclogites from southwestern Oregon: Geological Society of America Bulletin, v. 84, n. 8, p. 2471–2488, https://doi.org/10.1130/0016-7606(1973)84<2471:EFSO>2.0.CO;2

Ghent, E. D., Coleman, R. G., and Hadley, D. G., 1980, Ultramafic inclusions and host alkali olivine basalts of the southern coastal plain of the Red Sea, Saudi Arabia: American Journal of Science, v. 280-A, The Jackson Volume, Part 2, p. 499–527.

Gooley, J. T., Grove, M., and Graham, S. A., 2021a, Tectonic evolution of the central California margin as reflected by detrital zircon composition in the Mount Diablo region, *in* Sullivan, R., Sloan, D., Unrah, J. R., and Schwartz, D. P., editors, Regional Geology of Mount Diablo, California: Its Tectonic Evolution on the North America Plate Boundary: Geological Society of America Memoir, v. 217, p. 305–329, https://doi.org/10.1130/2021.1217(14)

Gooley, J. T., Sharman, G. R., and Graham, S. A., 2021b, Reconciling along-strike disparity in slip displacement of the San Andreas fault, central California, USA: Geological Society of America Bulletin, v. 133, n. 7–8, p. 1441–1464, https://doi.org/10.1130/B35681.1

Graham, S. A., 1987, Tectonic controls on petroleum occurrence in central California, *in* Ingersoll, R. V., and Ernst, W. G., editors, Cenozoic basin development of coastal California: Englewood Cliffs, New Jersey, Prentice-Hall, p. 47–63.

Graham, S. A., and Berry, K. D., 1979, Early Eocene paleogeography of the central San Joaquin Valley: Origin of the Cantua Sandstone: Tertiary Symposium Volume, Pacific Section, Society Economic Paleontologists and Mineralogists, p. 119–127.

Graham, S. A., and Williams, L. A., 1985, Tectonic, depositional, and diagenetic history of Monterey Formation (Miocene), central San Joaquin basin, California: American Association Petroleum Geologists Bulletin, v. 69, n. 3, p. 385–411, https://doi.org/10.1306/AD4624F7-16F7-11D7-8645000102C1865D

Graham, S. A., McCloy, C., Hitzman, M., Ward, R., and Turner, R., 1984, Basin evolution during change from convergent to transform continental margin in central California: American Association of Petroleum Geologists Bulletin, v. 68, n. 3, p. 233–249, https://doi.org/10.1306/AD460A03-16F7-11D7-8645000102C1865D

Graham, S. A., Stanley, R. G., Bent, J. V., and Carter, J. B., 1989, Oligocene and Miocene paleogeography of central California and displacement along the San Andreas fault: Geological Society of America Bulletin, v. 101, n. 5, p. 711–730, https://doi.org/10.1130/0016-7606(1989)101<0711:OAMPOC>2.3.CO;2

Graymer, R. W., Langenheim, W. E., Roberts, M. A., and McDougall, K., 2014, Geological and geophysical maps of the eastern three-fourths of the Cambria 30’x60’ Quadrangle, central California Coast Ranges: U.S. Geological Survey, Scientific Investigation Map 3287, scale 1:100,000, https://doi.org/10.3133/sim3287

Griscom, A., and Jachens, R. C., 1990, Tectonic implications of gravity and magnetic models along east-west seismic profiles across the Great Valley near Coalinga: U.S. Geological Survey, Professional Paper, v. 1487, p. 69–78.

Guzofski, C. A., Shaw, J. H., Lin, G., and Shearer, P. M., 2007, Seismically active wedge structure beneath the Coalinga anticline, San Joaquin basin, California: Journal of Geophysical Research: Solid Earth, v. 112, n. B3, B03S05, https://doi.org/10.1029/2006JB004465

Harding, T. P., 1976, Tectonic significance and hydrocarbon trapping consequences of sequential folding synchronous with San Andreas faulting, San Joaquin Valley, California: American Association of Petroleum Geologists Bulletin v. 60, n. 3, p. 356–378, https://doi.org/10.1306/83D923C0-16C7-11D7-8645000102C1865D

Harrison, J. C., 1995, Tectonics, kinematics of foreland folded belt influenced by salt, Arctic Canada, *in* Jackson, M. P. A., Roberts, D. G., and Snelson, S., editors, Salt tectonics: A global perspective: American Association of Petroleum Geologists, Memoir, v. 65, p. 379–412, https://doi.org/10.1306/M65604C19

Herzberg, C., 2004, Geodynamic information in peridotite petrology: Journal of Petrology v. 45, n. 12, p. 2507–2530, https://doi.org/10.1093/petrology/egh039

Hickman, S., and Langbein, J., 2004, The Parkfield Experiment–Capturing what happens in an Earthquake: US Geological Survey, Fact Sheet 049-02, https://doi.org/10.3133/fs04902

Hopson, C. A., Mattinson, J. M., and Pessagno, E. A., 1981, Coast Range ophiolite, western California: Englewood Cliffs, New Jersey, Prentice-Hall, p. 418–510.

Horodyskyj, U., Lee, C. A., and Luffi, P., 2009, Geochemical evidence for exhumation of eclogite via serpentinite channels in ocean-continent subduction zones: Geosphere, v. 5, n. 5, p. 426–438, https://doi.org/10.1130/GES00502.1

Hudec, M. R., and Jackson, M. P. A., 2012, De Re Salsa: Fundamental principles of salt tectonics, *in* Roberts, D. G., and Bally, A. W., editors, Regional Geology and Tectonics: Phanerozoic Passive Margins, Cratonic Basins and Global Tectonic Map: Elsevier, p. 18–41, https://doi.org/10.1016/B978-0-444-56357-6.00001-9

Ingersoll, R. V., 1982, Initiation and evolution of the Great Valley forearc basin of northern and central California, U.S.A., *in* Leggett, J. K., editor, Trench-Forearc Geology: Sedimentation and Tectonics on Modern and Ancient Active Plate Margins: Geological Society, London, Special Publication, v. 10, p. 459–467, https://doi.org/10.1144/GSL.SP.1982.010.01.31

Irwin, W. P., 1977, Ophiolitic terranes of California, Oregon, and Nevada: State of Oregon Department of Geology and Mineral Industry Bulletin, v. 95, p. 75–92.

Jachens, R. C., Griscom, A., and Roberts, C. W., 1995, Regional extent of Great Valley basement west of the Great Valley, California: Implications for extensive tectonic wedging in the California Coast Ranges: Journal of Geophysical Research: Solid Earth, v. 100, n. B7, p. 12769–12790, https://doi.org/10.1029/95JB00718

Jackson, M. P. A, Cornelius, R. R., Craig, C. H., Gansser, A., Stöcklin, J., and Talbot, C. J., 1990, Salt diapirs of the Great Kavit, central Iran: Geological Society of America, Memoir, v. 177, 139 p., https://doi.org/10.1130/MEM177-p1

Johnson, C. J., Bloch, R. B., and Graham, S. A., 2005, Tertiary sequences of the central San Joaquin Basin, California: Age control and eustatic versus tectonic forcing factors: Pacific Section American Association of Petroleum Geologists, Miscellaneous Publications Series 49.

Johnson, C. L., and Graham, S. A., 2007, Middle Tertiary stratigraphic sequences of the San Joaquin basin, California, *in* Scheirer, H. A., editor, Petroleum Systems and Geologic Assessment of Oil and Gas in the San Joaquin Basin Province, California: U.S. Geological Survey, Professional Paper 1713-6, https://doi.org/10.3133/pp17136

Johnson, P. A., and McEvilly, T. V., 1995, Parkfield seismicity: Fluid-driven?: Journal of Geophysical Research: Solid Earth, v. 100, n. B7, p. 12,937–12,950, https://doi.org/10.1029/95JB00474

Kuespert, J., 1985, Depositional environments and sedimentary history of the Miocene Temblor Formation and associated Oligo-Miocene units in the vicinity of Kettleman North Dome, San Joaquin Valley, California, *in* Graham, S. A., editor, Geology of the Temblor Formation, western San Joaquin basin, California: Pacific Section, Society Economic Paleontologists and Mineralogists, v. 44, p. 53–68

Laurs, B. M., Rohtert, W. R., and Gary, M., 1997, Benitoite from the New Idria District, San Benito County, California: Gems and Gemology, v. 33, n. 3, p. 166–187, https://doi.org/10.5741/GEMS.33.3.166

Lazar, C., Cooperdock, E. H. G., and Seymour, B. H. T., 2021, A contininental forearc serpentinite diapir with deep origins: Elemental signatures of a mantle wedge protolith and slab-derived fluids at New Idria, California: Lithos, v. 389–399, https://doi.org/10.1016/j.lithos.2021.106252

Letouzey, J., Colletta, B., Vially, R., and Chermette, J. C., 1995, Evolution of salt-related structures in compressional settings, *in* Jackson, M. P. A., Roberts, D. G., and Snelson, S., editors, Salt tectonics: A global perspective: American Association of Petroleum Geologists, Memoir, v. 65, p.41–60, https://doi.org/10.1306/M65604C3

Lockwood, J. P., 1971, Sedimentary and gravity-slide emplacement of serpentinite: Geological Society of America Bulletin, v. 82, n. 4, p. 919–936, https://doi.org/10.1130/0016-7606(1971)82[919:SAGEOS]2.0.CO;2

Loney, R. A., Himmelberg, G. R., and Coleman, R. G., 1971, Structure and petrology of the Alpine-type peridotite at Burro Mountain, California, U.S.A.: Journal of Petrology, v. 12, n. 2, p. 245–309, https://doi.org/10.1093/petrology/12.2.245

Lowell, R. P., and Rona, P. A., 2002, Seafloor hydrothermal systems driven by the serpentinization of peridotite: Geophysical Research Letters, v. 29, n. 11, p. 26-1–26-4, https://doi.org/10.1029/2001GL014411

Martin, B., and Fyfe, W. S., 1970, Some experimental and theoretical observations on the kinetics of hydration reactions with particular reference to serpentinization: Chemical Geology, v. 6, p. 185–202, https://doi.org/10.1016/0009-2541(70)90018-5

Mattinson, J. M., 1986, Geochronology of high-pressure-low-temperature Franciscan metabasites: A new approach using the U-Pb system, *in* Evans, B. W., and Brown, E. H. editors, Blueschist and eclogites: Geological Society of America, Memoirs, v. 164, p. 95–105, https://doi.org/10.1130/MEM164-p95

Mattinson, J. M.1988, Constraints on the timing of Franciscan metamorphism: Geochronlogical approaches and their limitations, *in* Ernst, W. G., editor, Metamorphism and crustal evolution of the western United States: Prentice-Hall, Englewood Cliffs, New Jersey, Rubey, v. 7, p. 1023–1034.

Mattinson, J. M., and Echeverria, L. M., 1980, Ortigalita Peak gabbro, Franciscan complex-U-Pb ages of intrusion and high pressure-low temperature metamorphism: Geology, v. 8, n. 12, p. 589–593, https://doi.org/10.1130/0091-7613(1980)8<589:OPGFCU>2.0.CO;2

Mattinson, J. M., and Hopson, C.A., 1992, U/Pb ages of the Coast Range ophiolite: A critical revaluation based on new high-precision Pb/Pb ages: American Association of Petroleum Geologists Bulletin, v. 76, p. 425.

McDougall, K., 2007, California Cenozoic biostratigraphy: Paleogene, in Petroleum systems and geologic assessment of oil and gas in the San Joaquin Basin, California: US Geological Survey, Professional Paper 1713, Ch. 4, p. 1–56.

McGuire, D., 1988a, Stratigraphy, depositional history, and hydrocarbon source-rock potential of the Upper Cretaceous-lower Tertiary Moreno Formation, central San Joaquin basin, California: PhD thesis, Stanford University, Stanford, 309 p.

McGuire, D. J., 1988b, Depositional framework of the Upper Cretaceous-lower Tertiary Moreno Formation, central San Joaquin Basin, California, *in* Graham, S. A., and Olson, H. C., editors, Studies of the geology of the San Joaquin Basin: Pacific Section, Society of Economic Paleontologists and Mineralogists, Book 60, p. 173–188.

McLaughlin, R. J., Sliter, W. V., Sorg, D. H., Russell, P. C., and Sarna-Wojcicki, A. M. 1996, Large-scale slip displacement on the East San Francisco Bay Region fault system, California: Implications for location of the late Miocene to Pliocene Pacific Plate Boundary: Tectonics, v. 15, n. 1, p. 1–15, https://doi.org/10.1029/95TC02347

McPhee, D. K., Jachens, R. C., and Wentworth, C. M., 2004, Crustal structure across the San Andreas Fault at the SAFOD site from potential field and geologic studies: Geophysical Research Letters, v. 31, n. 12, L12S03, https://doi.org/10.1029/2003GL019363

Melson, W. G., Hart, S. R., and Thompson, G., 1972, St Paul's Rocks Equatorial Atlantic: petrogenesis, radiometric ages, and implications on sea-floor spreading. Geological Society of America, Memoir, v. 132, p. 241–272, https://doi.org/10.1130/MEM132-p241

Mevel, C., 2003, Serpentinization of abyssal peridotites at mid-ocean ridges: Comptes Rendus Geosciences, v. 335, n. 10–11, p. 825–852, https://doi.org/10.1016/j.crte.2003.08.006

Miller, D. D., and Graham, S. A., 2018, Late Cenozoic uplift and shortening in the central California coast ranges and development of the San Joaquin basin foreland, *in* Ingersoll, Lawton, R. V. T. F., and Graham, S. A., editors, Tectonics, Sedimentary Basins, and Provenance: A Celebration of the Career of William R. Dickinson: Geological Society of America, Special Paper, v. 540, p. 425–4450, https://doi.org/10.1130/2018.2540(19)

Mitchell, C., Graham, S. A., and Suek, D. H., 2010, Subduction complex uplift and exhumation and its influence on Maastrichtian forearc stratigraphy in the Great Valley basin, northern San Joaquin Valley, California: Geological Society of America Bulletin, v. 122, n. 11–12, p. 2063–2078, https://doi.org/10.1130/B30180.1

Moody, J. B., 1976, Serpentinization: a review: Lithos 9, n. 2, p. 125–138, https://doi.org/10.1016/0024-4937(76)90030-X

Moore, D. E., and Blake, M. C. Jr, 1989, New evidence of polyphase metamorphism of glaucophane schist and eclogite exotic blocks and the Franciscan Complex, California and Oregon: Journal of Metamorphic Geology, v. 7, n. 2, p. 211–226, https://doi.org/10.1111/j.1525-1314.1989.tb00585.x

Moore, D. E., and Lockner, D. A., 2013, Chemical controls on fault behavior: Weakening of serpentinite sheared against quartz-bearing rocks and its significance for fault creep in the San Andreas system: Journal of Geophysical Research: Solid Earth, v. 118, n. 5, p. 2558–2570, https://doi.org/10.1002/jgrb.50140

Moore, D. E., and Rymer, M. J., 2007, Talc–bearing serpentinite and the creeping section of the San Andreas fault: Nature, v. 448, p.795–797, https://doi.org/10.1038/nature06064

Mumpton, F. A., and Thompson, C. S., 1975, Mineralogy and origin of the Coalinga asbestos deposit: Clays and Clay Minerals, v. 23, p. 131–143, https://doi.org/10.1346/CCMN.1975.0230209

Murata, K. J., Dibble, T. W. Jr., and Drinkwater, J. L., 1979, Thermal effects of large bodies of intrusive serpentinite on overlying Monterey shale, southern Diablo Range, Cholame area, California: Geological Survey, Professional Paper, 1082, p. 1–8, https://doi.org/10.3133/pp1082

Namson, J. S., and Davis, T. L., 1988, Seismically active fold and thrust belt in the San Joaquin Valley, central California: Geological Society of America Bulletin, v. 100, n. 2, p. 257–273, https://doi.org/10.1130/0016-7606(1988)100<0257:SAFATB>2.3.CO;2

Namson, J. S., Davis, T. L., and Lagoe, M. B., 1990, Tectonic history and thrust-fold deformation style of seismically active structures near Coalinga: U.S. Geological Survey, Professional Paper, v. 1487, p. 79–96.

Nilsen, T. H., and Dibblee, T. W. Jr., 1979, Geology of the central Diablo Range between Hollister and New Idria, California: Cordilleran Section, Geological Society of America, 106 p.

Nilsen, T. H., and Moore, D. W., 1997, Regional Upper Cretaceous stratigraphy and depositional systems of the northern San Joaquin Basin, California, *in* Knauer, L. C., editor, Geology of the northern San Joaquin Basin gas province: Bakersfield, California., Pacific Section American Association of Petroleum Geologists, MP 43, p. 1–12, https://doi.org/10.32375/1997-MP43.1

Nilsen, T. H., Dibblee, T. W. Jr., and Simoni, T. R. Jr., 1974, Stratigraphy and sedimentology of the Cantua Sandstone Member of the Lodo Formation, Vallecitos Area, California: Pacific Section SEPM, p. 38–68.

Normand, C., and Williams-Jones, A. E., 2007, Physicochemical conditions and timing of rodingite formation: evidence from rodingite-hosted fluid inclusions in the JM asbestos mine, Asbestos, Quebec: Geochemical Transactions, v. 8, 11, https://doi.org/10.1186/1467-4866-8-11

Obradovich, J. D., Kunk, M. J., and Lanphere, M. A., 2000, Age and paragenesis of the unique mineral Benitoite: Geological Society of America Absract with Programs, Annual Meeting 2000, v. 32, n. 7, p. 440.

Orme, D. A., and Graham, S. A., 2018, Four-dimensional model of Cretaceous depositional geometry and sediment flux in the northern Great Valley forearc, California, *in* Ingersoll, R. V., Lawton, T. F., and Graham, S. A., editors, Tectonics Sedimentary Basins, and Provenance: A Celebration of the Career of William R. Dickinson: Geological Society of America, Special Paper, v. 540, p. 409–424, https://doi.org/10.1130/2018.2540(18)

Page, B. M., and Brocher, T. M., 1993, Thrusting of the central California margin over the edge of the Pacific plate during the transform regime: Geology, v. 21, n. 7, p. 635–638, https://doi.org/10.1130/0091-7613(1993)021<0635:TOTCCM>2.3.CO;2

Page, B. M., Coleman, R. G., and Thompson, G. A., 1998, Overview: Cenozoic tectonics of the central and southern Coast Ranges, California: Geological Society of America Bulletin, v. 110, n. 7, p. 846–876, https://doi.org/10.1130/0016-7606(1998)110<0846:OLCTOT>2.3.CO;2

Platt, J. P., Xia, H., and Schmidt, W. L., 2018, Rheology and stress in subduction zones around the aseismic/seismic transition: Progress in Earth and Planetary Science, v. 5, 24, https://doi.org/10.1186/s40645-018-0183-8

Rentschler, M. S.,1985, Structurally controlled Neogene sedimentation in the Vallecitos syncline, *in* Graham, S. A., editor, Geology of the Temblor Formation, western San Joaquin basin, California: Pacific Section, Society Economic Paleontologists and Mineralogists, v. 44, p. 97–120.

Rentschler, M. S., and Bloch, R. B., 1988, Flexural subsidence modeling of the Tertiary San Joaquin Basin, California: Pacific Section SEPM, p. 29–52.

Reynard, B., Hilariet, N., Balan, E., and Lazzeri, M., 2007, Elasticity of serpentines and extensive serpentinization in subduction zones: Geophysical Research Letters. v. 34, n. 13, L13307, https://doi.org/10.1029/2007GL030176

Robertson, A. H. F., 1989, Paleoceanography and tectonic setting of the Jurassic Coast Range ophiolite, central California: evidence from extrusive rocks and the volcano clastic sediment cover: Marine and Petroleum Geology, v. 6, n. 3, p. 194–219, https://doi.org/10.1016/0264-8172(89)90001-9

Roland, E., Behn, M. D., and Hirth, G., 2010, Thermal-mechanical behavior of oceanic transform faults: Implications for the spatial distribution of seismicity: Geochemistry, Geophysics, Geosystems. v. 11, n. 7, Q07001, https://doi.org/10.1029/2010GC003034

Ross, M., and Nolan, R. P., 2003, History of asbestos discovery and use and asbestos-related disease in context with the occurrence of asbestos within ophiolite complexes, *in* Dilek, Y., and Newcomb, S., editors, Ophiolite concept and the evolution of geological thought: Geological Society of America, Special Paper, v. 373, p. 447–470, https://doi.org/10.1130/0-8137-2373-6.447

Rouméjon, S., and Cannat, M., 2014, Serpentinization of mantle-derived peridotites at mid-ocean ridges: Mesh texture development in the context of tectonic exhumation: Geochemistry, Geophysics, Geosystems, v.15, n. 6, p. 2354–2379, https://doi.org/10.1002/2013GC005148

Ryder, I., and Bürgmann, R., 2008, Spatial variations in slip deficit on the central San Andreas fault from InSAR: Geophysical Journal International, v. 175, p. 837–852, https://doi.org/10.1111/j.1365-246X.2008.03938.x

Rymer, M. J., and Ellsworth, W. L., 1990, The Coalinga, California, earthquake of May 2, 1983: U.S. Geological Survey, Professional Paper, v. 1487, 417 p., https://doi.org/10.3133/pp1487

Sans, M., and Vergés, J., 1995, Fold development related to contractional salt tectonics, southeastern Pyrenean thrust front, Spain, *in* Jackson, M. P. A., Roberts, D. G., and Snelson, S., editors, Salt tectonics: A global perspective: American Association of Petroleum Geologists, Memoir, v. 65, p.369–378, https://doi.org/10.1306/M65604C18

Scheirer, A. S., and Magoon, L. B., 2006, Age, distribution, and stratigraphic relationship of rock units in the San Joaquin basin province, California, *in* Scheirer, A. H., editor, Petroleum systems and geologic assessment of oil and gas in the San Joaquin Basin, California: US Geological Survey, Professional Paper, v. 1713, Ch. 5, p. 1–107.

Schulein, B. J., ms, 1993, Sedimentation and tectonics of the upper lower to lower middle Eocene Domengine Formation, Vallecitos syncline, California: M.S. thesis, Stanford University, Stanford, 343 p.

Sharman, G. R., Graham, S. A., Grove, M., and Hourigan, J. K., 2013, A reappraisal of the early slip history of the San Andreas fault, central California, USA: Geology, v. 41, n. 7, p. 727–730, https://doi.org/10.1130/G34214.1

Sharman, G. R., Schwartz, T. M., Shumaker, L. E., Trigg, C. R., Nieminski, N. M., Sickmann, Z. T., Malkowski, M. A., Hourig., J. K., Schulein, B. J., and Graham, S. A., 2017, Submarine mass failure within the deltaic Domengine Formation (Eocene), California (USA): Geosphere, v. 13, n. 3, p. 950–973, https://doi.org/10.1130/GES01442.1

Shibakusa, H., and Maekawa, H., 1997, Lawsonite-bearing eclogite metabasite in the Cazadero area, California: Mineralogy and Petrology v. 61, p. 163–180, https://doi.org/10.1007/BF01172482

Stein, R. S., and King, G. C. P., 1984, Seismic potential revealed by surface folding: 1983 Coalinga, California, earthquake: Science, v. 224, n. 4651, p. 869–871, https://doi.org/10.1126/science.224.4651.869

Stock, J., and Molnar, P., 1988, Uncertainties and implications of the Late Cretaceous and Tertiary position of North America relative to the Farallón, Kula, and Pacific plates: Tectonics, v. 7, n. 6, p. 1339–1384, https://doi.org/10.1029/TC007i006p01339

Suzuki, Y., 1986, Melange problem of convergent plate margins in the Circum Pacific Regions: Kochi, Japan, Memoirs of the Faculty of Science, Kochi University, Series E, Geology v. 7, p. 23–48.

ten Brink, U. S., Shimizu, N., and Molzer, P. C., 1999, Plate deformation at depth undernorthern California: Slab gap or stretched slab?: Tectonics, v. 18, n. 6, p. 1084–1098, https://doi.org/10.1029/1999TC900050

Titus, S. J., Medaris, L. G. Jr., Wang, H. F., and Tikof, B., 2007, Continuation of the San Andreas fault system into the upper mantle: Evidence from spinel peridotite xenoliths in the Coyote Lake basalt, central California: Tectonophysics, v. 429, n. 1–2, p. 1–20, https://doi.org/10.1016/j.tecto.2006.07.004

Titus, S. J., Dyson, M., DeMets, C., Tikoff, B., Rolandone, F., and Bürgmann, R., 2011, Geologic versus geodetic deformation adjacent to the San Andreas fault, central California: Geological Society of America Bulletin, v. 12, n. 5–6, p. 790–820, https://doi.org/10.1130/B30150.1

Tsujimori, T., Liou, J. G., and Coleman, R. G., 2007a, Finding of high-grade tectonic blocks from the New Idria serpentine body, Diablo Range, California: Petrologic constraints on the tectonic evolution of an active serpentine diapir: Geological Society of America, Special Paper, v. 419, p. 67–80, https://doi.org/10.1130/2007.2419(03)

Tsujimori, T., Moriguti, T., Kunihiro, K., Kobayashi, K., and Nakkamura, E., 2007b, Large-scale fluid flow in a cold subduction-zone: STMS Li-isotope study of jadeite veins in Franciscan metagraywacke: Goldschmidt Conference Abstract 2007, p. A1040.

Ukar, E., Cloos, M., and Vasconcelos, P., 2012, First ^{40}Ar-^{39}Ar ages from low-T mafic blueschist blocks in a Franciscan melange near San Simeon: Implications for initiation of subduction: Journal of Geology, v. 120, n. 5, p. 543–556, https://doi.org/10.1086/666745

Van Baalen, M. R.,1993, Titanium mobility in metamorphic systems: a review: Chemical Geology, v. 110, n. 1–3, p. 233–249, https://doi.org/10.1016/0009-2541(93)90256-I

Vermeesch, P., Millar, D. D., Graham, S. A., and De Grave, J., 2006, Multimethod detrital thermochronology of the Great Valley Group near New Idria, California: Geological Society of America Bulletin, v. 118, n. 1–2, p. 210–218, https://doi.org/10.1130/B25797.1

Wakabayashi, J., 2015, Anatomy of a subduction complex: Architecture of the Franciscan complex, California, at multiple length and time scales: International Geology Review, v 57, n. 5–8, p. 609–746, https://doi.org/10.1080/00206814.2014.998728

Wakabayashi, J., Ghatak, A., and Basu, A. R., 2010, Suprasubduction-zone ophiolite generation, emplacement, and initiation of subduction: A perspective from geochemistry, metamorphism, geochronology, and regional geology: Geological Society of America Bulletin, v. 122, n. 9–10, p. 1548–1568, https://doi.org/10.1130/B30017.1

Walter, A. W., 1990, Upper-crustal velocity structure near Coalinga, as determined from seismic-refraction data: U.S. Geological Survey, Professional Paper, v. 1487, p. 23–40.

Warren, J. M., 2016, Global variations in abyssal peridotites compositions: Lithos, v. 248–251, p. 191–219, https://doi.org/10.1016/j.lithos.2015.12.023

Watt, J. T., Ponce, D. A., Graymer, R. W., Jachens, R. C., and Simpson, R. W., 2014, Subsurface geometry of the San Andreas-Calaveras fault junction: Influence of serpentinite and the Coast Range Ophiolite: Tectonics, v. 33, n. 10, p. 2025–2044, https://doi.org/10.1002/2014TC003561

Wentworth, C. M., 1990, Structure of the Coalinga region and thrust origin of the earthquake: U.S. Geological Survey, Professional Paper, v. 1487, p. 41–68.

Wentworth, C. M., and Zoback, M. D., 1989, The style of late Cenozoic deformation in the eastern front of the California Coast Ranges: Tectonics, v. 8, n. 2, p. 237–246, https://doi.org/10.1029/TC008i002p00237

Wentworth, C. M., and Zoback, M. D., 1990, Structure of the Coalinga area and thrust origin of the earthquake: U. S. Geological Survey, Professional Paper, v. 1487, p. 47–68

Wentworth, C. M., Blake, M. C. Jr., Jones, D. L., Walter, A. W., and Zoback, M. D., 1984, Tectonic wedging associated with emplacement of the Franciscan assemblage, California Coast Ranges, *in* Blake, M. C. J., editor, Franciscan geology of northern California: Pacific Section, Society of Economic Paleontologists and Mineralogists, v. 43, p. 163–173.

Wentworth, C. M., Jachens, R. C., Simpson, R. W., and Michael, A. J. 1992, Structure of the Parkfield region, CA, from geology and geophysics compiled in a Geographic Information system: American Geophysical Union, 1992 Fall Meeting abstracts, supplement to Eos, v. 73, n. 43, p. 396.

Wentworth, C. M., Jachens, R.C., Simpson, R.W., and Michael, A.J., 1993, Structure of the Parkfield region, CA, from geology and geophysics compiled in a Geographic Information System (1:250,000 scale maps): US Geological Survey Open File.

Woodring, W. P., Stewart, R. B., and Richards, R. W., 1940, Geology of the Kettleman Hills: U.S. Geological Survey, Professional Paper, v. 195, 170 p.

Yerkes, R. F., Levine, P., and Wentworth, C. M., 1990, Abnormally high fluid pressures in the region of the Coalinga earthquake sequence and their significance, *in* Rymer, M. J., and Ellsworth, W. L., editors, The Coalinga Earthquake of May 2, 1983: U.S. Geological Survey, Professional Paper, v. 1487, p. 35–257.

Zharikov, V. A., Pertsev, N. N., Rusinov, V. L., Callegari, E., and Fettes, D. J., 2007, Metasomatism and metasomatic rocks, *in* Fettes, D., and Desmons, J., editors, Metamorphic Rocks–A classification and glossary of terms: IUGS Subcommission on Systematics of Metamorphic Rocks: Cambridge University Press, p. 58–68.